POLITEHNICA UNIVERSITY OF BUCHAREST
Doctoral School of Chemical Engineering and Biotechnologies

PhD THESIS SUMMARY

CONTRIBUTIONS REGARDING THE STUDY OF THE BEHAVIOR OF CR THIN LAYER DEPOSITIONS ON THE ZIRCALOY-4 ALLOY, UNDER HIGH PRESSURE AND TEMPERATURE CONDITIONS

Scientific adviser:

Prof. Univ. Dr. Ioana DEMETRESCU

PhD student:

Diana AȘTEFĂNESEI (DINIASI)

Bucharest

2024

Acknowledgements,

With great respect,

Diana Diniasi

Introduction

Zirconium - based alloys are in present used as cladding materials for fuel rods in the nuclear reactors due to the small neutron cross section, good corrosion resistance and mechanical properties. During a LOCA accident, the temperature of the cladding can exceed 800 °C, oxidation reactions and hydrogen generation being significantly accelerated. The consequences of such reaction were oberved during the Fukushima-Daichi accident [1], [2].

These problems have led the nuclear industry to focus some of its efforts on increasing the operational safety of current nuclear reactors and improving the safety of future types of reactors. A promising approach that has generated considerable research interest is the development of protective coatings or surface treatments of materials that would improve the oxidation resistance of the zirconium alloy cladding to be more tolerant to degradation under LOCA conditions. Thus, if the degradation of the cladding is delayed it will increase the response time in the event of an accident. Furthermore, this direction could have the advantage of reducing the oxidation rate and hydrogen uptake during normal operation, leading to increased overall reactor safety [3].

Although the nuclear power industry is based on a mature technology with an excellent record of safe operation and the current fuel, UO_2, meets all the performance and safety requirements, keeping nuclear power as a clean and economically competitive energy option, in the recent years, important directions have been drawn regarding the development of accident-tolerant materials (ATF), aiming to increase the safety and competitiveness of current nuclear power plants [4].

This paper addresses a research direction of great topicality and interest, being included in most research and development programs in the field of nuclear energy, and has as ***general objective*** the analysis of the corrosion mechanism of chromium coatings deposited on the Zy-4 substrate and the study of their corrosion performance on long term. Experimental research program consisted in testing and investigating the corrosion behavior of nuclear fuel cladding material, Zy-4 alloy, with improved anti-corrosion properties by applying a metallic chromium-based diffusion barrier layer.

Specific objectives were established:
1. Development of protective metallic chromium coatings by physical deposition methods;
2. Morphological and structural characterization and evaluation of the anticorrosive performances of the Cr coating;
3. Long-term testing of the performance of the coating in an aqueous environment, at high temperature and pressure, in static autoclaves;
4. Morphological and structural characterization and anticorrosive performance evaluation of post-autoclaving Cr coating.

The doctoral thesis entitled ***" Contributions regarding the study of the behavior of the deposition of thin layers of Cr on the Zircaloy-4 alloy, under high pressure and temperature conditions"*** comprises a theoretical part, an experimental part and a final part with general conclusions, the further research directions and the scientific contributions of the author in the research field of this project.

In chapter 1, ***"The current stage of scientific research on the deposition of thin layers on metal alloys with applications in the nuclear field"*** , a literature review of the most representative studies on the use of zirconium alloys in the nuclear field was carried out, being detailed discussed

the kinetics and corrosion mechanism of zirconium alloys, the factors that influence the corrosion behavior of zirconium alloys, the oxidation mechanism of zirconium alloys, the mechanism of hydrogen absorption and hydride formation. Also, a literature review was carried out regarding the nationally and internationally research in the field of accident-tolerant materials, with the focus on the development and testing of metallic chromium coatings, deposited on zirconium alloy substrate. The requirements and challenges regarding the deposition of coatings on zirconium alloys with applications in the nuclear field, the current state in the development of thin films on the substrate of zirconium alloys, the evaluation of their performances, degradation mechanisms of the coating and methods to improve the resistance to corrosion have been discussed. Also, a methodology was defined for the technical evaluation of the accident-tolerant materials candidate as cladding materials.

Chapter 2, *"Materials and experimental methodology"*, includes a detailed presentation of the deposition methods, the corrosion testing equipment for the Cr coating, as well as the post - corrosion chromium deposition characterization techniques: the gravimetric analysis, the metallographic analysis, X-ray diffraction, scanning electron microscopy, X-ray fluorescence, electrochemical techniques (open circuit potential variation, electrochemical impedance spectroscopy and linear potentiodynamic polarization).

In chapter 3, *" Experimental research on the corrosion behavior of the Zy-4 alloy deposited with a thin film of Cr, in water at high temperature and pressure"* , the applied experiments, the obtained results and their interpretation are presented. The original experimental research has investigated and evaluated the anticorrosive properties of the metallic chromium coating provided to the Zy-4 alloy. Chapter 3 is structured in 2 subchapters as follows:

-   In Subchapter 3.1, the experimental researches and the results obtained regarding the morphological and structural characterization of the as-coated Cr samples, as well as the evaluation of the corrosion behavior, are described. The investigation of the crystalline structure of the coating, the determination of the thickness of the deposited Cr layer, the elemental composition of the coating, as well as the identification of possible defects in the deposited films were achieved.

-   In Subchapter 3.2, the experimental researches and the results obtained regarding the corrosion testing of the coated Cr Zy-4 alloy are presented. Corrosion testing of the samples was carried out in a 1l static autoclave, in an aqueous environment, simulating the primary circuit conditions in a CANDU nuclear reactor. Subsequently, post-corrosion samples were characterized by gravimetric analysis, metallographic analysis, SEM/EDS analyses, X-ray diffraction method , XPS analysis. Corrosion susceptibility assessment was also carried out by electrochemical methods such as: EIS analysis, open circuit corrosion potential measurements and linear potentiodynamic polarization.

In Chapter 4, *"Conclusions and recommendation for future work"*, the general conclusions on the experimental results presented in the doctoral thesis in the field of development, testing and analysis of the long-term performance of metallic Cr coatings deposited on Zy-4 substrate are presented.

In Chapter 5, *" Personal contributions and scientific achievements in the field of doctoral study "*, are presented the author's contributions in the field of doctoral study as well as scientific achievements that reflects the elements of originality of the project.

2 MATERIALS AND EXPERIMENTAL METHODOLOGY

In this chapter, the experimental methods used to achieve the goals of this thesis are presented in detail. In the beginning, the substrate preparation stage, preliminary to the deposition stage, is presented, as well as the three physical deposition methods used to deposited the metallic Cr coatings: thermionic vacuum arc (TVA) method, electron beam physical vapor deposition (EBPVD) and magnetron sputtering (MS). The following is the description of the experimental test conditions at high pressure and temperature in water and the Cr-coated Zy-4 alloy. The chapter ends with the presentation of the characterization techniques and the associated experimental thesis plan.

Research program

The experimental research included in the present thesis has followed a work plan. In Fig. 2.1. is presented the associated experimental thesis work plan:
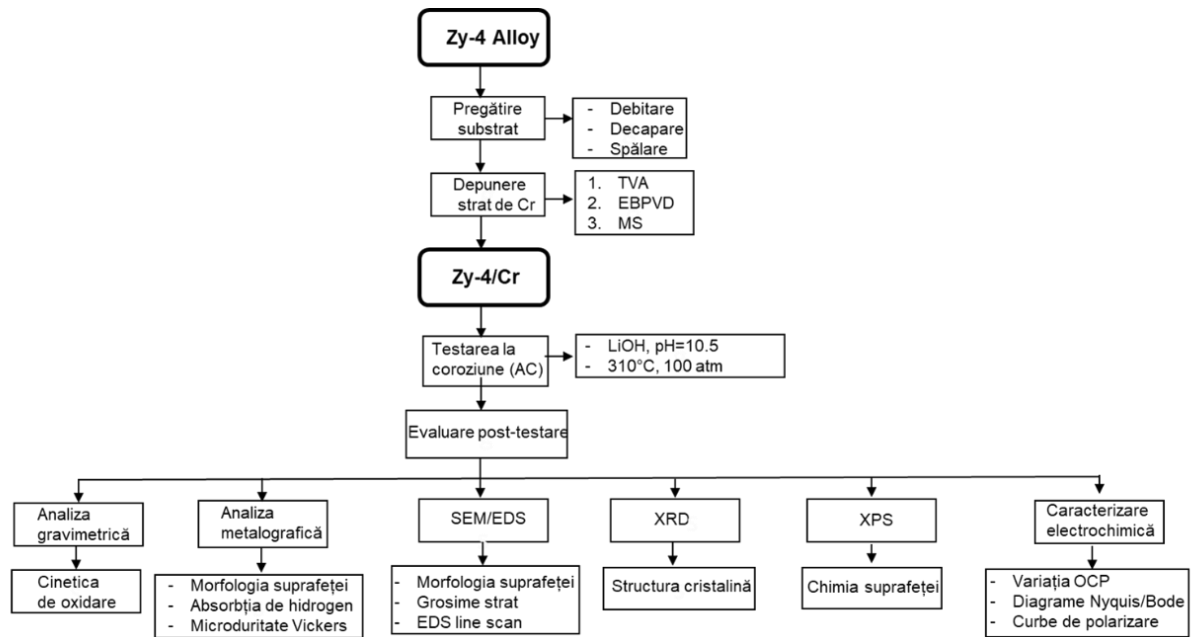
Fig. 2.1. The experimental work plan associated with the thesis

The work plan includes three parts: deposition process, corrosion testing of the coatings and characterization of the Cr coatings.

3 EXPERIMENTAL RESEARCH ON THE CORROSION BEHAVIOR OF ZY-4 ALLOY DEPOSITED WITH A THIN CR LAYER IN WATER, AT HIGH TEMPERATURE AND PRESSURE

3.1 Morphological and structural characterization of the as-coated Cr coatings. Evaluation of the corrosion behavior.

The performance of the Cr coated zirconium alloy it is influenced by the microstructure and properties of the coating, which also depends on the materials used for deposition and the parameters of the deposition process.

3.1.1 X-ray diffraction method

For the Cr coated Zy-4 samples, the results of qualitative phase analysis are presented as diffraction spectra in the figure 3.1.
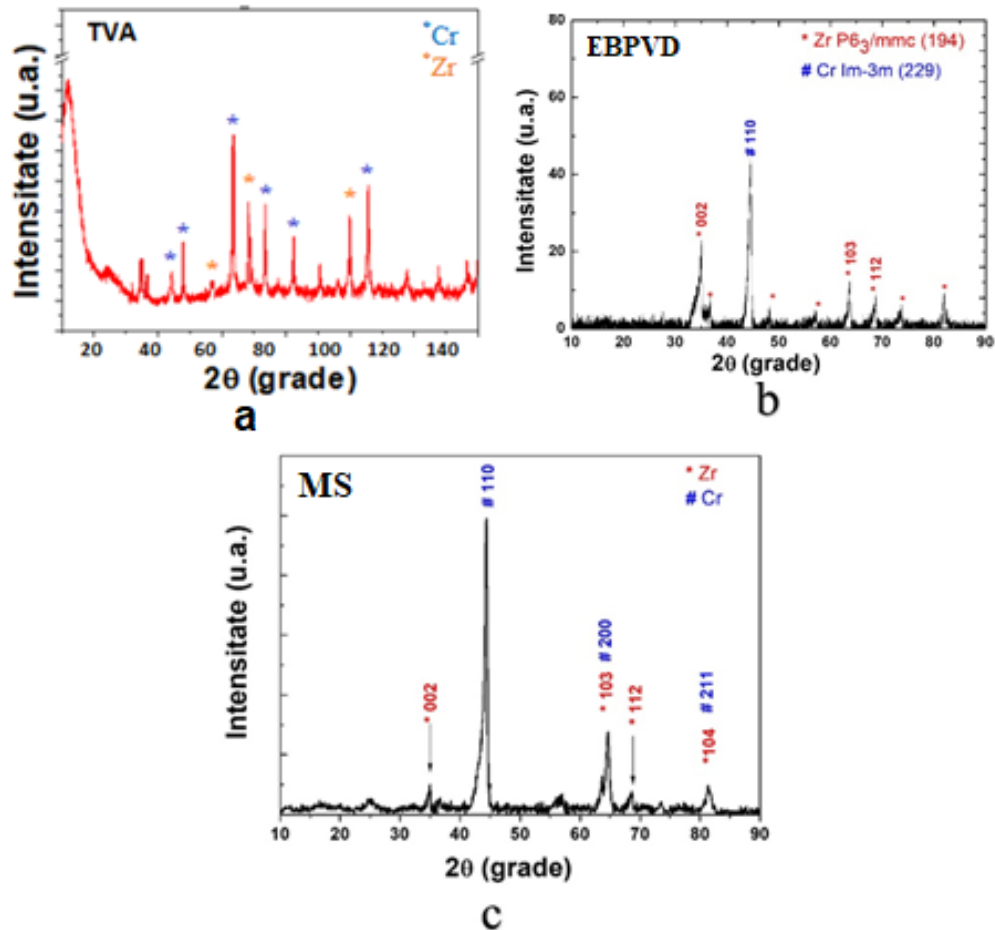
Fig. 3.1 XRD spectra for Zy-4 samples deposited by various physical deposition methods

It can be seen from the above figure the presence of two textured polycrystalline phases highlights by the presence of multiple diffraction peaks. It can be observed that the main phase

corresponding to metallic chrome, Im-3m space group, with a body-centered cubic arangement of atoms in the elemental lattice. The main hkl planes associated with the Cr phase (110), (200) and (211) with the main preferential crystalline growth on (110) plane. Compared to cristaline symmetry of Cr obtained in the specialized literature, in the present study the Cr nanocrystallites show an increase on the (200) orientation, compared to (211). This characteristic it is determined by the HiPIMS plasma parameters selected for Cr deposition. Another crystalline phase was identified, with a lower intensity of peaks compared cu Cr, corresponding to the substrate material, namely Zr, P63/mmc (194) space group with a hexagonal arangement of atoms in the elemental lattice.

3.1.2 Scanning electron microscopy

The thickness of the deposited Cr layer and the elemental composition of the coatings was determined. Also, it was investigated the presence of possible defects in coatings.

In Fig. 3.2. are presented the cross-section SEM images for the Zy-4 samples deposited with Cr by various physical methods.
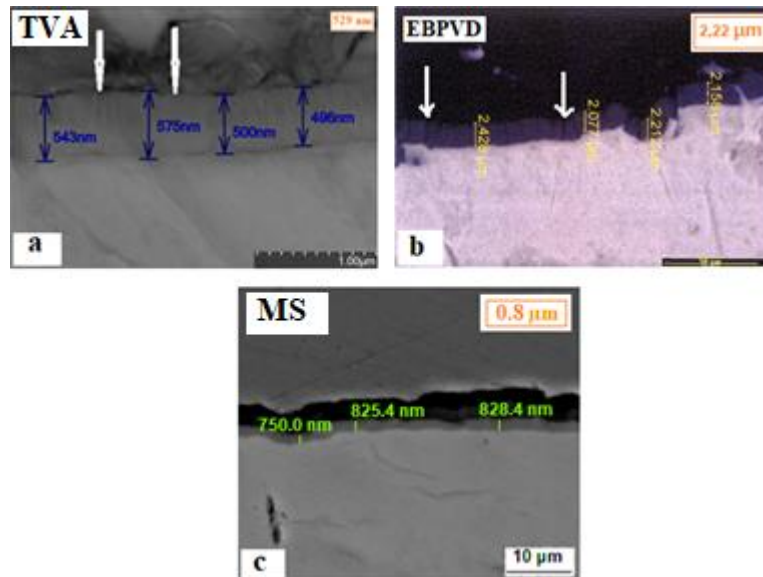
Fig. 3.2 Cross-section SEM micrographs for as-deposited Cr Zy-4 samples

From Fig. 3.2. can be noticed the presence of uniform coatings with average thicknesses of $0.53 \mu m$, $2.22 \mu m$, respectively $0.8 \mu m$, depending on the deposition method. The Cr coatings show a columnar structure [5],[6] and it was noted the presence of some fine cannelures (indicated by the arrows), without other visible defects.

Surface morphology of Cr coatings, along with their EDS analysis are presented in Fig. 3.3. Elemental distribution analysis confirms the presence of chromium in the highest concentration, as well as oxygen in small quantities.
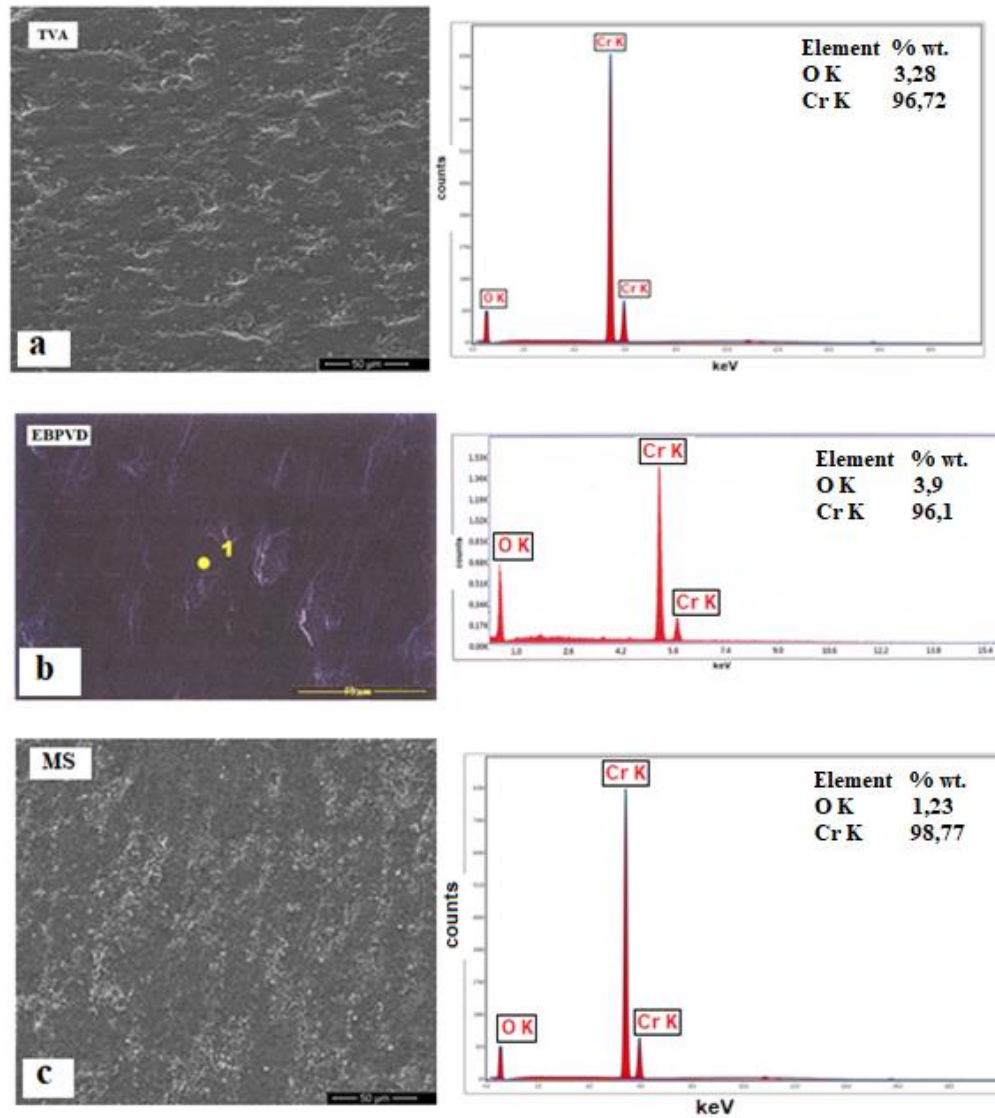
Fig. 3.3 SEM micrographs illustrating the surface morphology and related EDS spectra for Cr-coated Zy-4 samples

The elemental depth analysis of Cr coating, starting from the base material to surface, highlights the Cr increase as Zr decrease, Fig. 3.4.
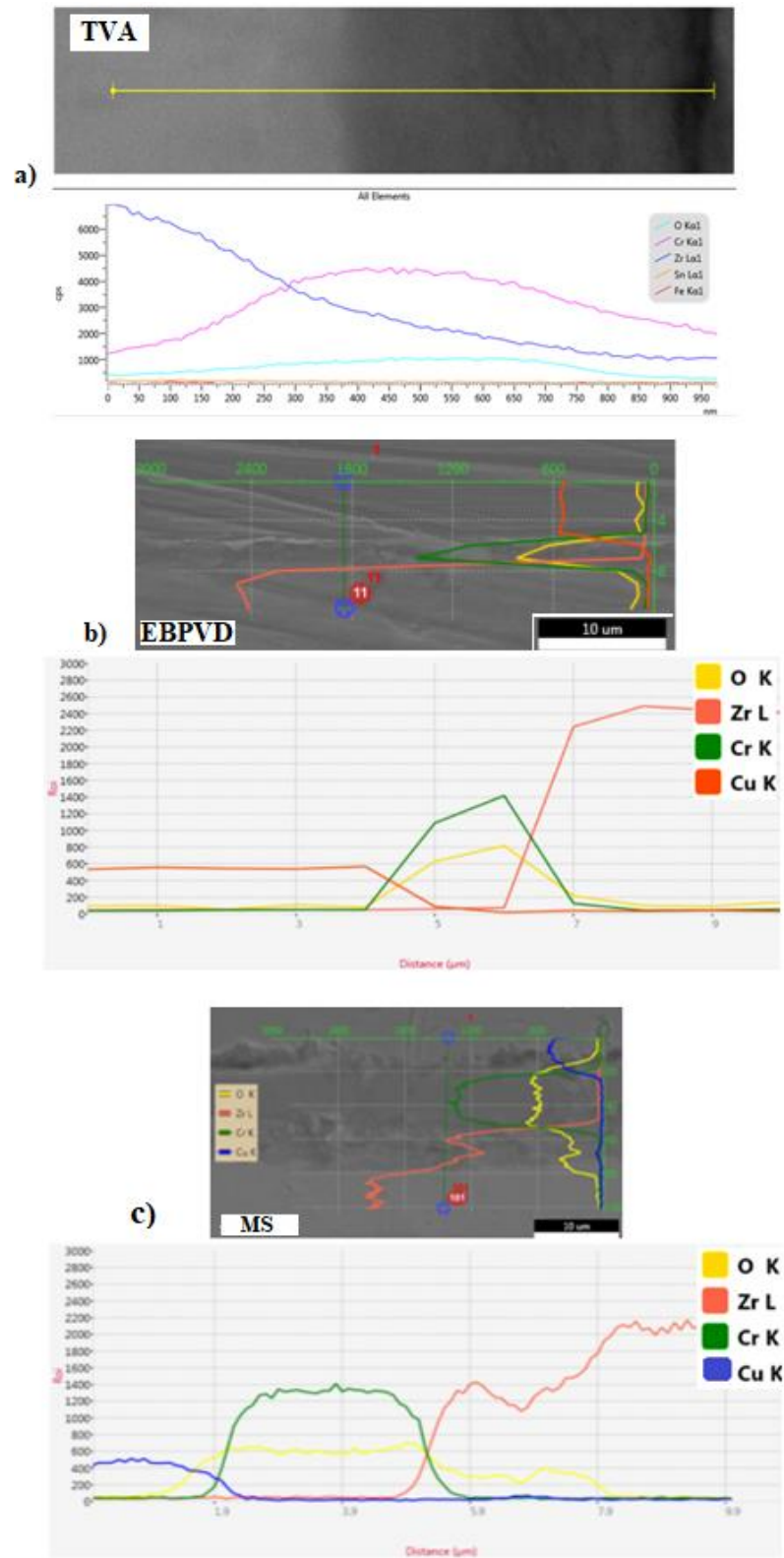
Fig. 3.4. EDS line scan analysis of the Cr layer deposited on the Zy-4 substrate by: a) TVA; b) EBPVD; c) MS

3.1.3 X - ray photoelectrons spectroscopy

The XPS measurements were performed to obtain information about surface chemistry and oxidation states of the detected elements.
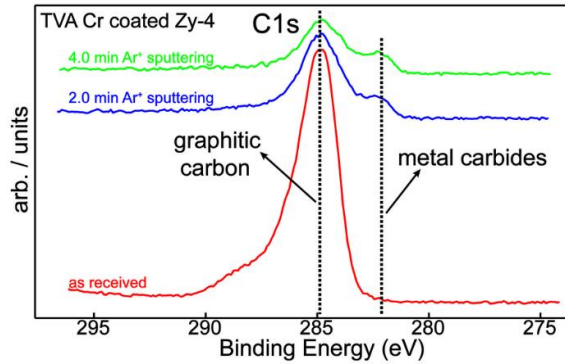
Fig. 3.5. C1s superimposed spectra before and after Ar$^+$ ion sputtering

Fig. 3.5. shows a decreasing graphitic contribution with the increase of the carbide feature after cleaning the surface by Ar$^+$ ion sputtering.

After deconvoluting the C1s photoelectron line, we can notice the chemical species labeled on the spectrum (Fig. 3.6.): oxidized carbon, C-C chemical bonding and carbides.
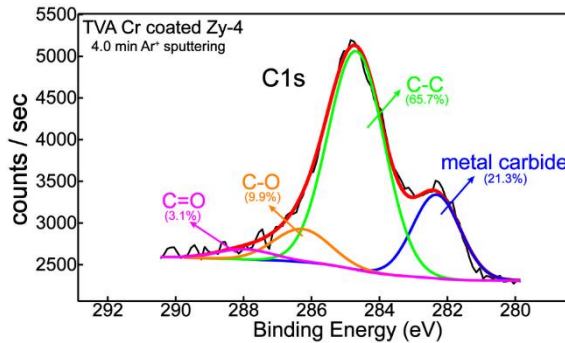
Fig.3.6. C1s XPS deconvoluted spectrum after 4.0 min Ar+ ion sputtering

For a general overview of the chromium chemical behavior, the spectra were selected and superimposed before and after sputtering (Fig. 3.7.). It can be seen that a dominant metallic contribution appears after 2.0 and 4.0 min Ar+ ion sputtering assessed by peak binding energy and line shape asymmetry. In the "as received" stage (before Ar+ ion sputtering), a mixture of oxidized and metallic chromium was detected.
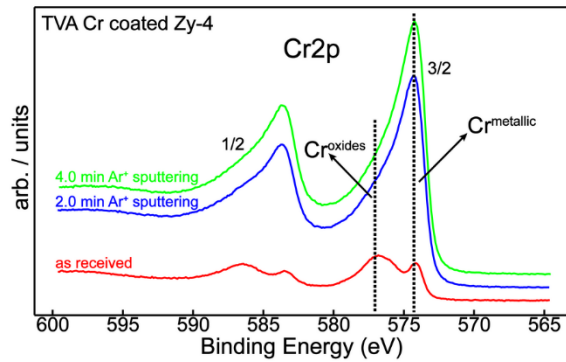
Fig. 3.7. Cr2p XPS superimposed spectra before and after Ar+ ion sputtering

The spectral deconvolution of Cr2p3/2 line was performed, in order to distinguish chromium chemical states (Fig. 3.8.). Therefore, Cr0 (metallic), Cr3+ (Cr2O3) and Cr6+ (CrO3) oxidation states together with chromium nitride were labeled on the spectrum. After 4.0 min Ar+ ion sputtering, the XPS signal was collected from the subsurface region, indicating an enriched metallic contribution (~75%), although a chemical interaction between nitrogen and chromium can be noticed.
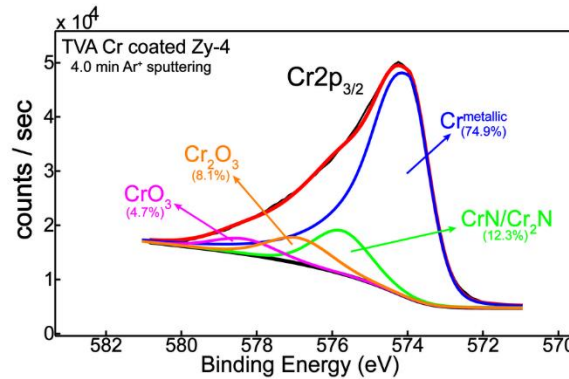
Fig.3.8. Cr2p3/2 XPS deconvoluted spectrum before and after Ar+ ion sputtering

The quantitative analysis (table 3.1.) illustrates a decreasing trend for carbon and oxygen with an increasing nitrogen and chromium, from surface to subsurface region.

Table 3.1. Element relative concentration (at. %)

Zy-4 /Cr_ TVA	C1s	O1s	N1s	Cr2p
Before Ar sputtering	56.4	31.7	2.4	9.5
2.0 min Ar$^+$ sputtering	22.5	25.4	12.5	39.6
4.0 min Ar$^+$ sputtering	14.2	23.3	16.5	46.0

The surface chemistry of nitrogen is in agreement with chromium chemistry. Therefore, the N1s superimposed spectra show the chemical modification between surface and subsurface, from adsorbed nitrogen on the surface to nitrides (Fig. 3.9.). Additionally, this was accompanied by nitrogen concentration increase, from 2% to 16% (Table 3.1.).
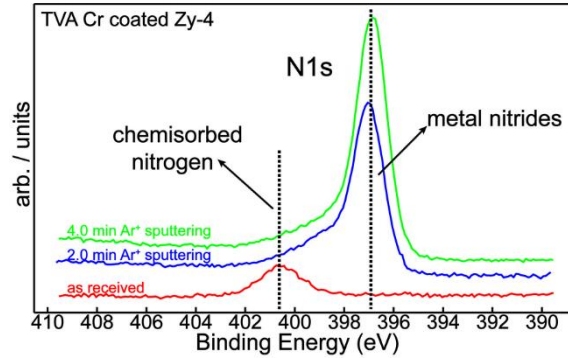
Fig.3.9. N1s XPS superimposed spectra before and after Ar+ ion sputtering

After peak-fitting the N1s signal (Fig. 3.10.), we can notice a dramatic decrease of chemisorbed nitrogen with an increase of chromium nitrides. The nitrides could be buried under carbon.
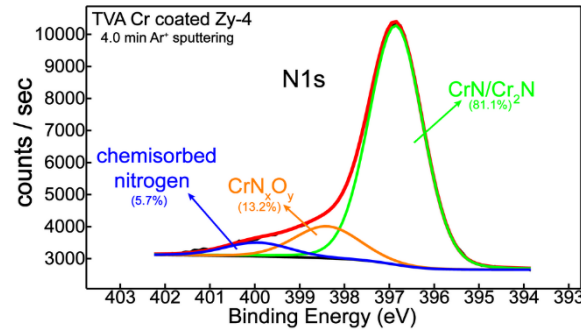
Fig.3.10. N1s XPS deconvoluted spectrum before and after Ar+ ion sputtering

3.1.4 Roughness measurements

Roughness determinations were applied on uncoated and coated samples. Due to the geometry of the Zy-4 sample, three measurements were made for each sample, both on the outer side of the sample and on the inner side. The average values of these measurements are shown in table 3.2.

Table 3.2 Average roughness measurements on uncoated and Cr coated Zy-4 samples

Sample	Side	Ra (µm)	Rmax (µm)	Rz (µm)
Zy-4	inner	0,487	5,27	4,31
	outer	0,476	3,87	3,27
Zy-4/Cr_TVA	inner	0,486	6,62	5,34
	outer	0,358	3,94	3,23
Zy-4/Cr_EBPVD	inner	0,416	5,35	4,11
	outer	0,458	3,38	3,2
Zy-4/Cr_MS	inner	0.413	5.77	4.24
	outer	0.268	4.03	3.27

Ra: average roughness
Rmax: maximum roughness depth
Rz: average maximum height of the profile

From 2D profiles analysis it can be obtained many roughness parameters, the most important being the average roughness parameter (Ra). Changes in surface morphologies caused by the applied deposition method are indicated by Ra parameter. The data summarized in the above tabel show smaller values of the roughness for all coated samples, compared to uncoated sample. Thus, we observe a slowly decrease of rougness value after Cr deposition. Because of the sample's geometry the surface of the material wasn't metallographic prepared. Accordingly, after Cr deposition the unevenness on the sample's surface have been covered and the roughness value decresed.

3.1.5 Electrochemical studies for corrosion susceptibility evaluation

3.1.5.1 Electrochemical impedance spectroscopy

By EIS it was realized a qualitative evaluation of the protective properties of the Cr coatings.

The Nyquist and Bode plots, Fig. 3.11., present the spectra recorded in open circuit, after 10 minutes of immersion in test solution of Cr - coated Zy-4 samples.
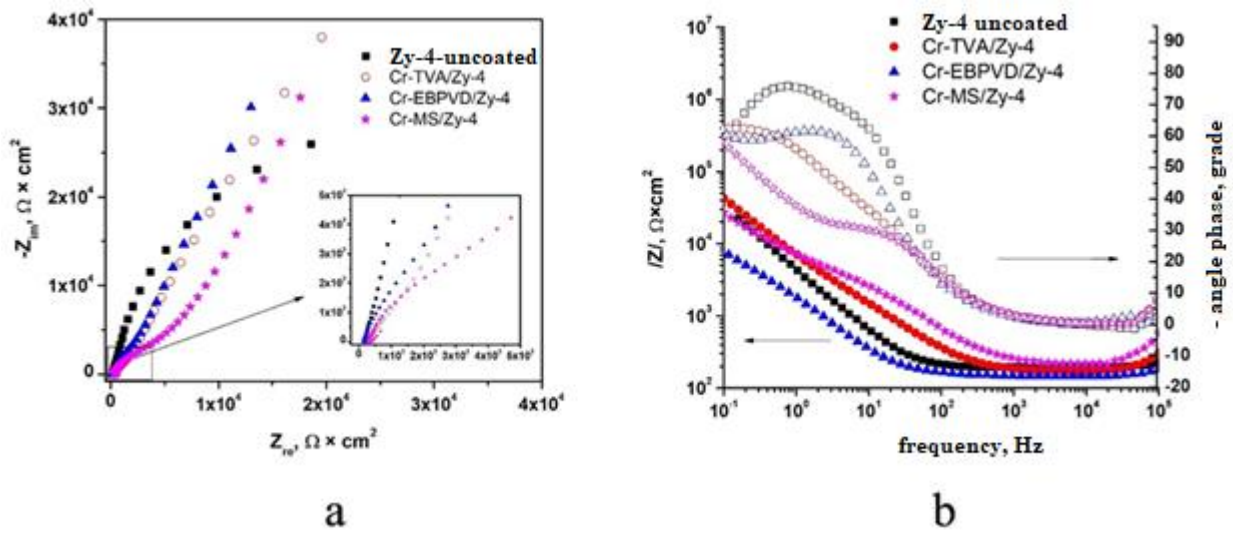
Fig.3.11. Superimposed diagrams for Cr coated Zy-4 samples: a) Nyquist; b) Bode |Z| and c) Bode Phase

As illustrating the Niquist diagram (Fig. 3.11. a) it is notice the presence of a single open capacitive semicircle for uncoated sample, while for the coated samples two open capacitive semicircles are identified, corresponding to that two interfaces created. Larger diameters values of the capacitive semicircles were also determined for the coated Zy-4 samples, compared to uncoated Zy-4 sample. This indicates higher polarization resistance values for the coated samples, which means better anticorrosion properties. Regular semicircles can also be observed, demonstrate the presence of uniform and smooth coatings.

Based on the Bode |Z| plots (Fig. 3.11. b) higher values of impedance were identified for the coated Zy-4 samples compared to uncoated sample. It is known that impedance magnitude, |Z|, is directly proportional to oxide resistance, so it can be concluded that these samples show higher corrosion resistance. These results are consistent with the lower corrosion rates calculated for the coated samples by potentiodynamic polarization.

The Bode Phase diagram (Fig. 3.11. b) indicate the existence of two maxima of the phase angle, one at high frequencies and the other at small frequencies. Higher value of the phase angle of the uncoated sample were observed, but it can be notice that at low frequencies the curve tends to zero while for the coated samples, after the curves reach a maximum the trend is to continue to increase. Phase angle values less than 90° have been recorded for both uncoated and coated samples, which means that the coatings are not totally capacitive.

3.1.5.2 Variation of open circuit corrosion potential

The generalized corrosion behaviour prediction for uncoated Zy-4 alloy and coated Zy-4 alloy was studied by applying open circuit potential measurements. A stable evolution of the potential can be observed, Fig. 3.12. Except for Cr coated Zy-4 by TVA, which shows a constant trend since the beginning of the test, the other samples present a stabilization of the potential after 600 s from immersion in electrolyte. Their later stabilization can be caused by electrolyte infiltration through the Cr coatings that cause reactions inside the coating. However, the

stabilization of the potential 600 s from the immersion confirms the fact that a passive oxide layer was formed on the analyzed surfaces.
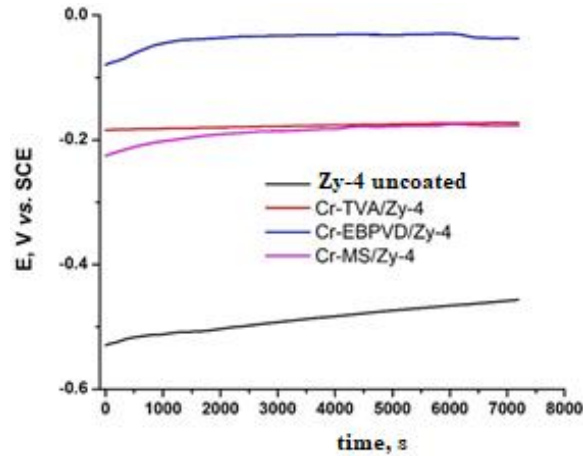
Fig. 3.12. Open circuit corrosion potential variation for uncoated and coated Zy-4 alloy

It is also noted that it does not exist high potential variations, indicating continuous and stable coatings.

In the table 3.3. are summarized the initial and the stabilized corrosion potential values for the tested samples.

Table 3.3. Corrosion potential values for uncoated and coated Zy-4 alloy

Sample	Zy-4	Zy-4/ Cr_TVA	Zy-4/ Cr_MS	Zy-4/Cr_EBPVD
Initial Ecorr (mV)	-530	- 182	- 225	- 82
Stabilized Ecorr (mV)	-464	- 172	- 175	- 37

3.1.5.3 Linear potentiodynamic polarization

The corrosion behaviour in CANDU reactor primary conditions was also evaluated by potentiodynamic polarization tests. In Fig. 3.13 are illustrated the potentiodynamic curves for uncoated and coated Zy-4.
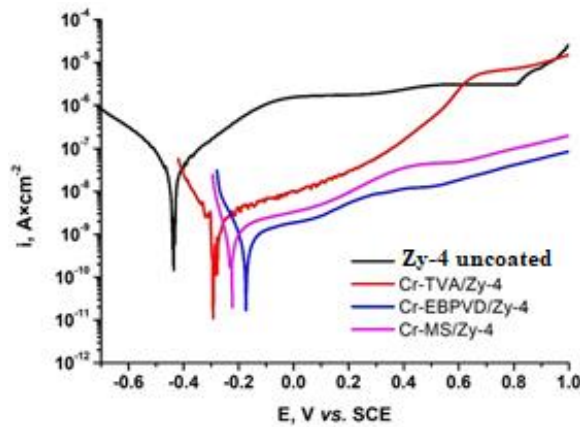
Fig.3.13. Comparative presentation of potentiodynamic polarization curves for uncoated and coated Zy-4 alloy

The curve trend show a pronounced thermodynamic tendency of corrosion for the uncoated Zy-4 (more electronegative value of Ecorr and higher corrosion current), compared to coated Zy-4 samples.

The electrochemical parameters specific to the corrosion process have been calculated appling two methods, Tafel extrapolation and polarization rezistance. They are: corrosion potential (Ecorr), corrosion rate (Vcorr), corrosion current (i_{corr}), polarization resistance (R_p), coating coefficient porosity (P) and coating protection efficiency (P_i).

Electrochemical parameters determined for tested samples are included in the table 3.4.

Table 3.4. Polarization parameters for uncoated and coated Zy-4 alloy

Sample	Metoda pantelor Tafel				Metoda rezistenței la polarizare		E, %	P (%)
	E_{cor}, mV	i_{cor}, nA×cm^{-2}	Kg, µg×m^{-2}h^{-1}	P, nm/an^{-1}	R_P, MΩ	i_{cor}, nA×cm^{-2}		
Zy-4	-436	190	3270	4360	0,26	179	-	-
Zy-4/Cr_TVA	−283	1,192	20,47	27,32	7,7	2,27	99,38	1,79×10^{-3}
Zy-4/Cr_EB-PVD	-167	0,586	10,08	13,45	48,1	0,543	99,69	3,11×10^{-5}
Zy-4/Cr_MS	-232	0,797	13,71	18,3	31,2	0,787	99,58	1,66×10^{-4}

Coating porosity coefficient and coating protection efficiency are two very important parameters for coating corrosion evaluation. The protection efficiency parameter allows us to appreciate the integrity of the coating, while a high coating porosity coefficient suggests a high density of defects on coatings surfaces [1].

Icorr values for coated and uncoated samples follow this order: Icorr_EBPVD << Icorr_TVA < Icorr_MS < Icorr_Zy-4 uncoated. As can be seen from Tabel, i_{corr} of uncoated Zy-4 is two orders of magnitude higher than corrosion current of the coated samples. Since i_{corr} is directly proportional to the material uniform corrosion rate result the Zy-4/Cr_EBPVD corrosion rate is lower than the other samples [7], [8].

3.2 Morphological and structural characterization of post-autoclaving Cr coatings. Evaluation of corrosion behavior.

In this chapter are presented the results of corrosion testing of Cr coated Zy-4 alloy after 504 h, 1512 h and respectively, 3024 h of exposure in the specific primary circuit conditions of a CANDU nuclear reactor (demineralized water with the addition of LiOH, pH = 10.5, T = 310 ° and p = 10 MPa). The analysis of Cr coating corrosion mechanism and long term corrosion behaviour represent the objectives of this chapter.

3.2.1 Metallographic analysis

Fig. 3.14. presents representative cross-section hydrides for chromium coated samples, as well as the density evolution of hydrides with autoclaving time. It can be observed a relatively uniform distribution of hydrides oriented along the circumferential plane of the samples.
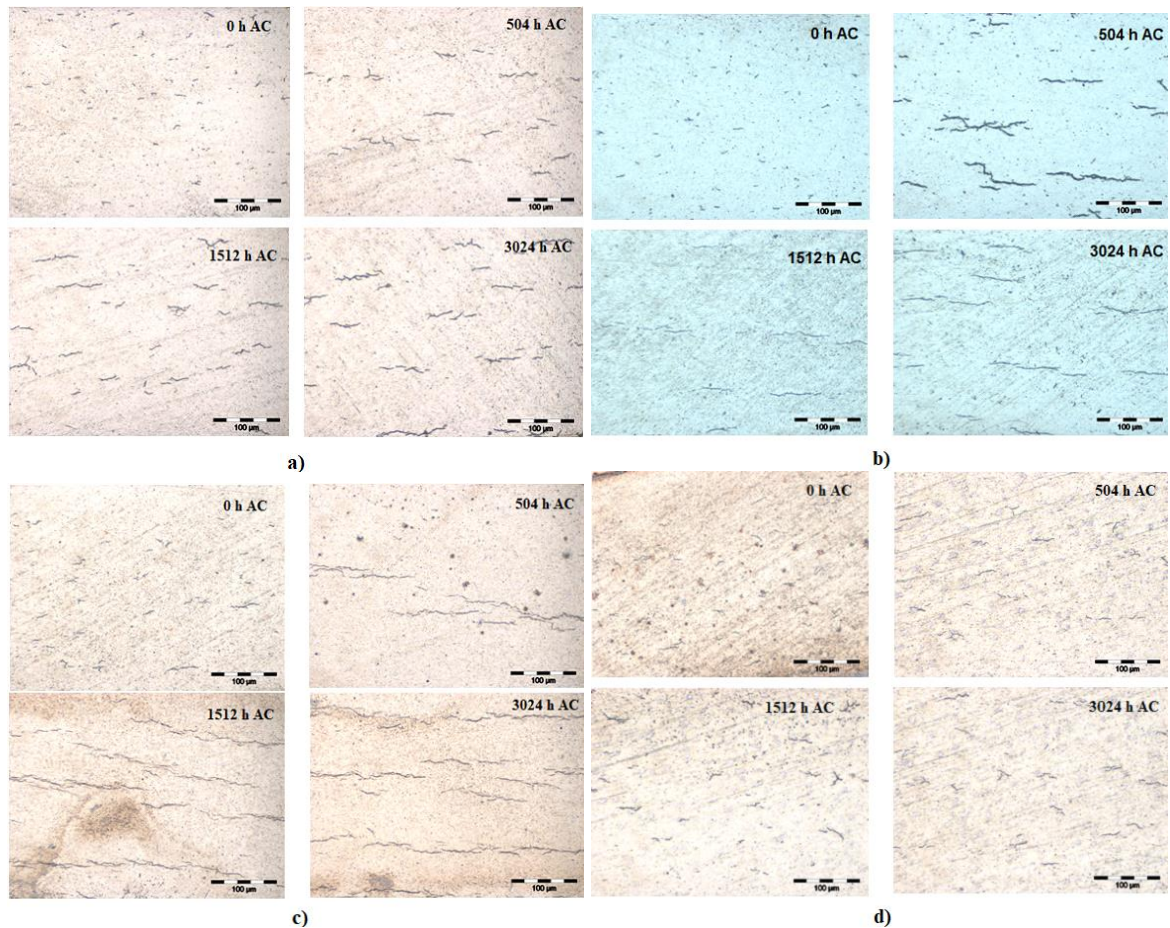
Fig.3.14. Representative hydrides and density evolution with autoclaving time: a) uncoated Zy-4; b) Cr coated Zy-4 by TVA; c) Cr coated Zy-4 by EBPVD; d) Cr coated Zy-4 by MS

Except for Cr coated Zy-4 by MS, an alignment of the hydrides was observed. This alignment is governed by hydride-hydride interactions (such as in sympathetic nucleation) or by hydrogen-hydride interactions (anisotropic growth), with the effect that hydrides tend to form in "bunches".

The surface morphologies of Zy-4 alloy samples coated with chromium and autoclaved various periods of time are presented as optical micrographs in Fig. 3.15.
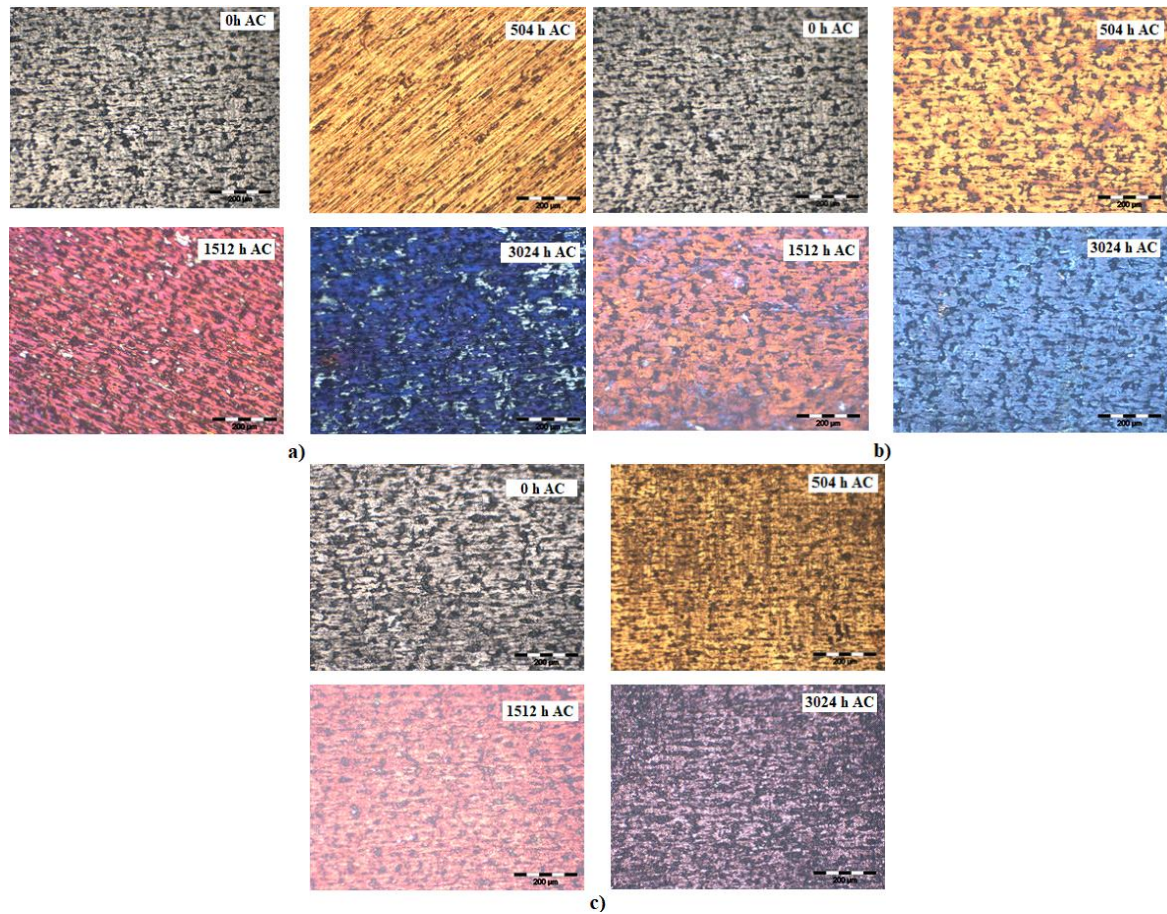
Fig. 3.15. Surface morphology for: a) Zy-4/Cr_TVA; b) Zy-4/Cr_EBPVD; c) Zy-4/Cr_MS, samples, autoclaved for various autoclaving periods

Based on the above micrographs, changes were identified in the coloration of the surface of the samples as the autoclaving time increased. The same colours are observed for all three tipes of coating, depending on the autoclaving time. The golden color suggests a very thin chromium oxide layer, while the shift to purple/bluish is given by the increase in chromium oxide layer thickness. According to the literature [10], the thickness of 100 nm is suggested by the micrograph's golden color, while for the purple/bluish color, a thickness of several hundreds of nanometers corresponds [9].

For the Vickers microhardness test (MHV0.1) was used a 0.1 Kgf load [10]. Since small differences were observed between the microhardness results at the substrate/coating interface and the middle of the samples, 10 indenter prints were made for each sample, 5 for each of the mentioned areas. Fig. 3.16. presents the average microhardness data for the tested samples.
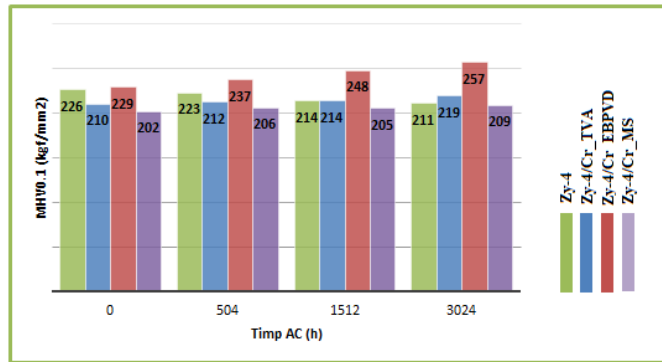
Fig.3.16. Variation of Vickers microhardness for post-autoclaved uncoated and coated Zy-4 samples

In the graph above the coated samples show a slight increase in microhardness values as autoclaving time increases. This behavior may indicate a tendency of the material to harden over time due to working conditions (high pressure and temperature, chemistry of testing solution) or because of the formation of zirconium hydrides, which may induce a material hardening effect [10].

3.2.2 Gravimetric analysis of Cr-coated Zy-4 alloy, autoclaved under primary circuit conditions

Weight gain measurements have been applied for five choosen samples, for each autoclaving time and deposition method, table 3.5. Based on these date all the coated samples show lower weight gain measurements compared to the uncoated Zy-4. The Zy-4/Cr_TVA presented the smallest values. During the autoclaving process there were no notable variations of weight measurements, the best stability having the Zy-4/Cr_EBPVD samples.

Also, we see that the data are consistent with coatings thicknesses measured by SEM.

Table 3.5. Average gain measurements for Cr coated Zy-4 autoclaved in the LiOH solution, at 310 °C and 10 MPa

Sample	Variația medie în greutate (mg x dm^{-2})	AC time, (h)					
		504	**1008**	**1512**	**2016**	**2520**	**3024**
Zy-4		10,31	11,03	14,36	16,39	16,46	17,75
Zy-4/Cr_TVA		3,75	4,25	4,45	4,65	4,9	5,1
Zy-4/Cr_EB-PVD		4,52	4,98	5,26	6,06	6,11	6,11
Zy-4/Cr_MS		4,02	4,53	4,71	5,05	5,13	5,56

Based on weight gains measurements corrosion kinetics was performed, represented by the mass gain as a function of exposure time, presented in Fig. 3.17.
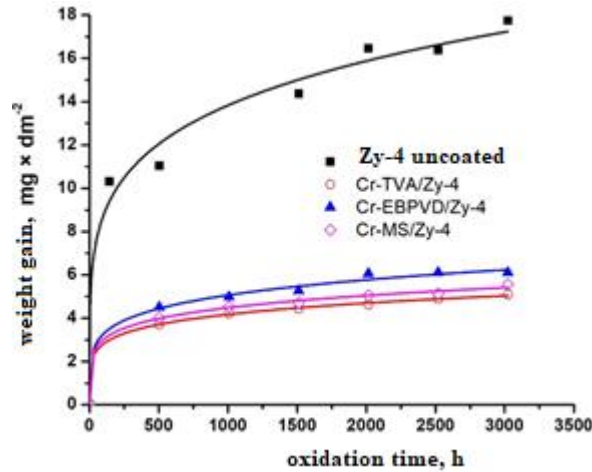
Fig. 3.17. Weight gain evolution for Cr coated Zy-4 samples autoclaved under primary circuit conditions.

Corrosion kinetics, both for uncoated and coated samples, follow a cubic law, in agreement with the data presented in other specialized studies [2], [3], [4], [5], [6], [7], [8]. [9]. The corrosion process is described by a power law, as follow:

$\Delta W = k_p * t^n$,

where, ΔW is the oxide weight (mg/dm^2), k_p the rate constant, t is the exposure time (h) and n is the exponent.

The oxidation constants, for each case, are presented in table 3.6.

Table 3.6. Parameters kinetics for the samples tested

Sample	$\Delta W = k_p * t^n$		
	k_p	n	R^2
Zy-4	3,49	0,199	0,987
Zy-4/Cr_TVA	1,286	0,170	0,999
Zy-4/Cr_EB-PVD	1,919	0,143	0,996
Zy-4/Cr_MS	1,376	0,167	0,997

Based on the data contained in the table above, a very good reliability factor can be observed for all the fits ($R^2 \sim 0.993 \div 0.999$). The kinetic parameters k_p and n show slightly different values depending on the coating method used. According to the specialized literature [10], [2], [11], [6] [7] [8], [9], are three types of laws, depending on n, as follows: n is close to 0.3 the corrosion process is described by a cubic law; if n is close to 0.5, the law is parabolic; n is close to 1, the law is linear. As can be seen from Table 3.6., for all coatings methods n is close to 0.3, accordingly the corrosion process is described by a cubic law [5].

It was observed that the corrosion rates decrease with the increase of the oxide layer, thus it can be stated that the transport of oxidizing species through the oxide layer controls the corrosion rate. In the present study, the role of Cr coating in slowing down the corrosion rate is demonstrated

by lower mass gain compared to uncoated Zy-4 alloy, as well as a stabilization of the mass gain after approximately 2000 h of corrosion testing.

3.2.3   Determination of surface morphology and elemental composition using SEM and EDS analyses

Figure 3.18. illustrates the surface morphology of Zy-4 samples coated with Cr by three physical deposition methods and autoclaved for various periods of time.
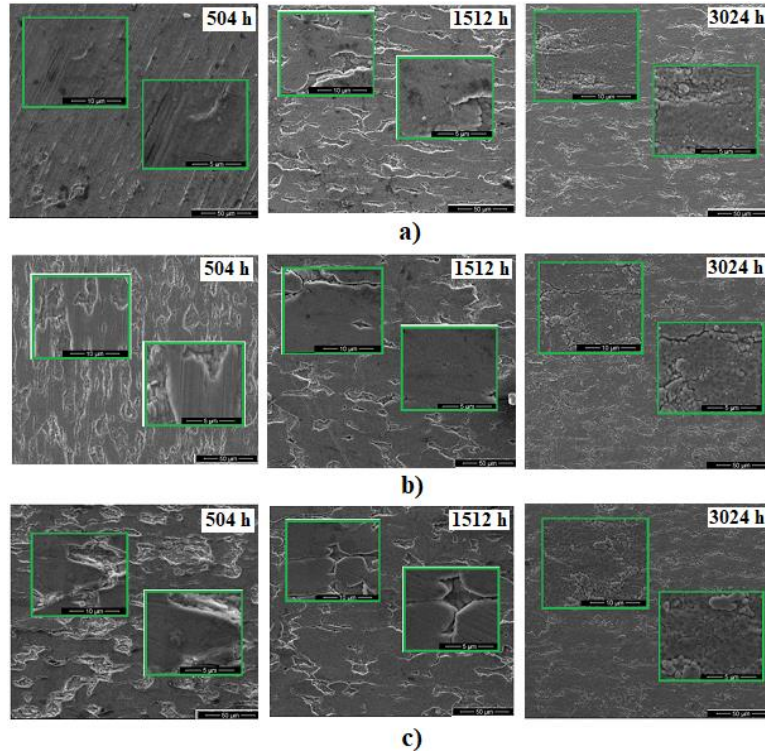
Fig.3.18. SEM surface morphology for Cr- coated Zy-4 samples after different autoclaving time

From Fig. 3.18. it can be observed that after every autoclaving period, the coating is still adherent, having a surface morphology like the as-received coating. There were not identified areas with delamination, loss of its integrity or presenting susceptibility to localized corrosion.

The elemental surface distribution of the samples is presented in the following, the EDS spectra and the concentrations for the elements of interest: chromium, zirconium and oxygen, are presented.

Set I - Zy-4/ Cr_TVA samples

For the Zy-4 samples coated with Cr by TVA method, the variation of the Cr, O and Zr concentration during the autoclaving period is ilustrated in Fig. 3.19.
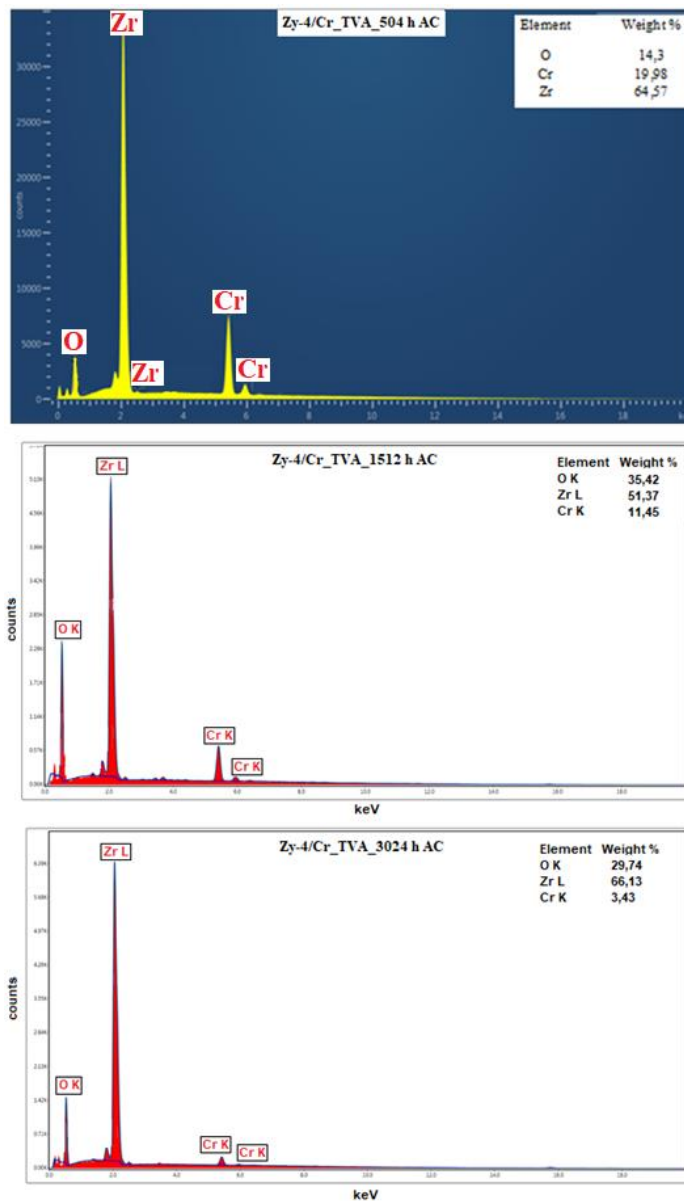
Fig. 3.19. EDS spectra for Zy-4 samples coated with Cr by TVA method and autoclaved various periods of time

After 504 h of autoclaving, a decrease in Cr concentration about 5 times was observed, compared to the as-coated sample. The downward trend of the chromium concentration continued, reaching a value of 11.45 % Cr after 1512 h of autoclaving, respectively 3.43 % Cr at the end of the autoclaving process. Similar to the concentration of chromium, the oxygen and zirconium concentrations presented very large variations after the first 504 h of autoclaving, the concentration of oxygen increasing by 12 times compared to the initial value (after coating and before autoclaving), and that of zirconium reaching the value of ~ 65 % Zr. After the next autoclaving cycle (1512 h) a slight increase in oxygen concentration and a decrease in Zr concentration were observed, while after 3024 h of autoclaving the reverse process was identified.

Set II - Zy-4/Cr_EBPVD samples

EDS analysis of the Cr coated Zy-4 samples by EBPVD method and autoclaved for different periods are included in Fig. 3.20. The results show a different evolution in the concentration of Cr, Zr and O elements, compared to the case of the samples deposited by TVA method.
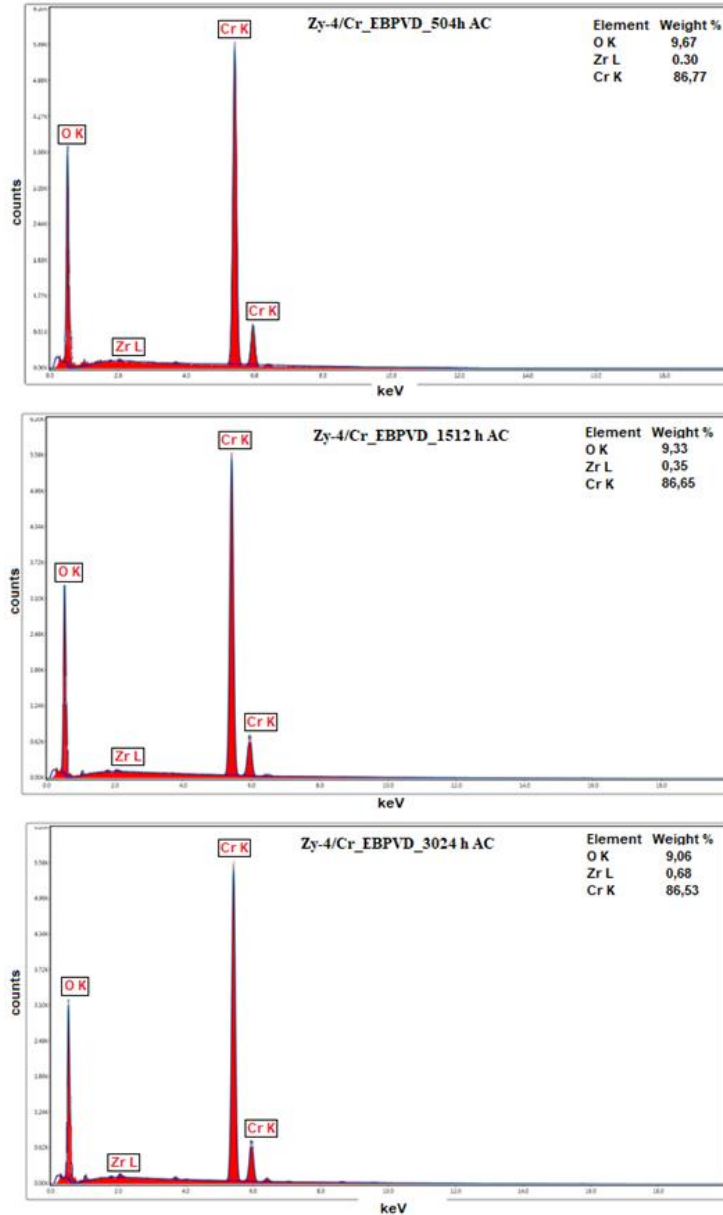
Fig. 3.20. EDS spectra for Zy-4 samples coated with Cr by EBPVD method and autoclaved various periods of time

As for the previous deposited samples, after the first autoclaving cycle (504 h), the largest variations in the concentration of the elements of interest are recorded: the concentration of oxygen increased by ~ 2.5 times compared to the initial value, that of chromium decreased by 10 percent, and zirconium reached a value of 0.3% Zr. However, during the next autoclaving time minor

variations in the concentration of the elements were recorded. Thus, it can be considered that this coating showed a higher stability under the autoclaving conditions.

Set III - Zy-4/ Cr_MS Samples

The investigation of elemental distributions performed on the Zy-4 samples coated with Cr by MS method was realised through EDS method. The recorded spectra are summarized in Fig. 3.21.
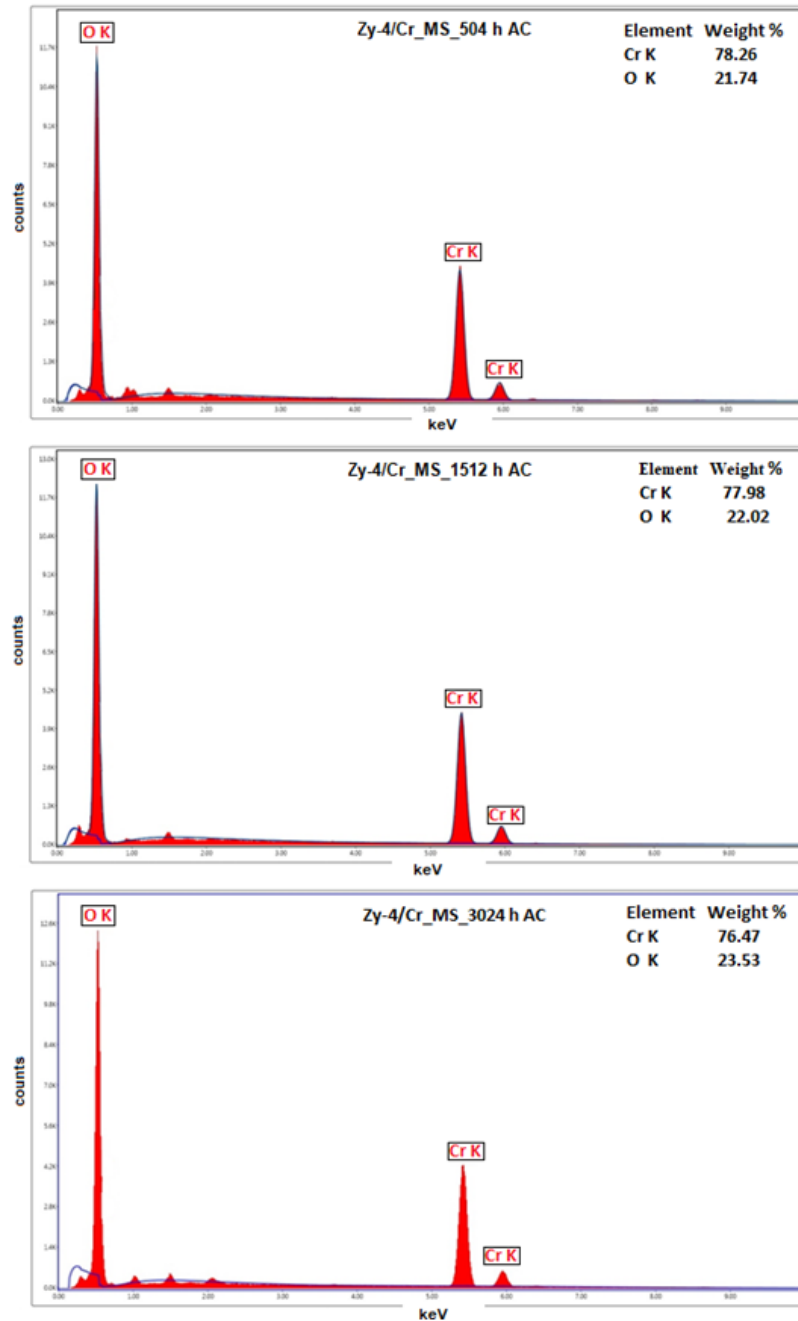
Fig. 3.21. EDS spectra for Zy-4 samples coated with Cr by MS method and autoclaved various periods of time

Based on the above spectra there were observed small variations of elements concentrations.

For a better understanding of Cr evolution during the autoclaving process, it was realized the graphic presented below, Fig. 3.22.
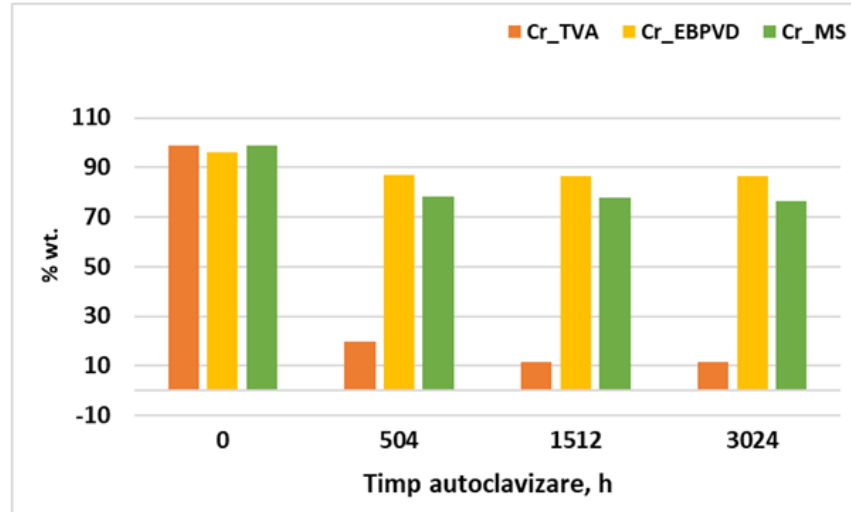
Fig. 3.22. The evolution of the Cr concentration during the autoclaving process

Tha data presented in the graphic from Fig. 3.25 show that even if the initial Cr concentration had very closed values for all three types of coatings, during the autoclaving process it evolution was very different, depending on the coating method. Thus, it is notable the Cr concentration decrease about 5 times after the first 504 h of autoclaving for Zy-4/Cr_TVA. Insignificant variations are seen for the Cr evolution in the case of the Zy-4/Cr_MS and Zy-4/Cr_EBPVD samples, the last one presented the best stability during the autoclaving process.

3.2.3.1   Cross section SEM-EDS analysis

Integrity assessment and outer layer thickness measurements were performed for Zy-4 samples coated with Cr and autoclaved for different periods of time. The cross-section SEM images, representative for the tested samples, are shown in Fig. 3.23.
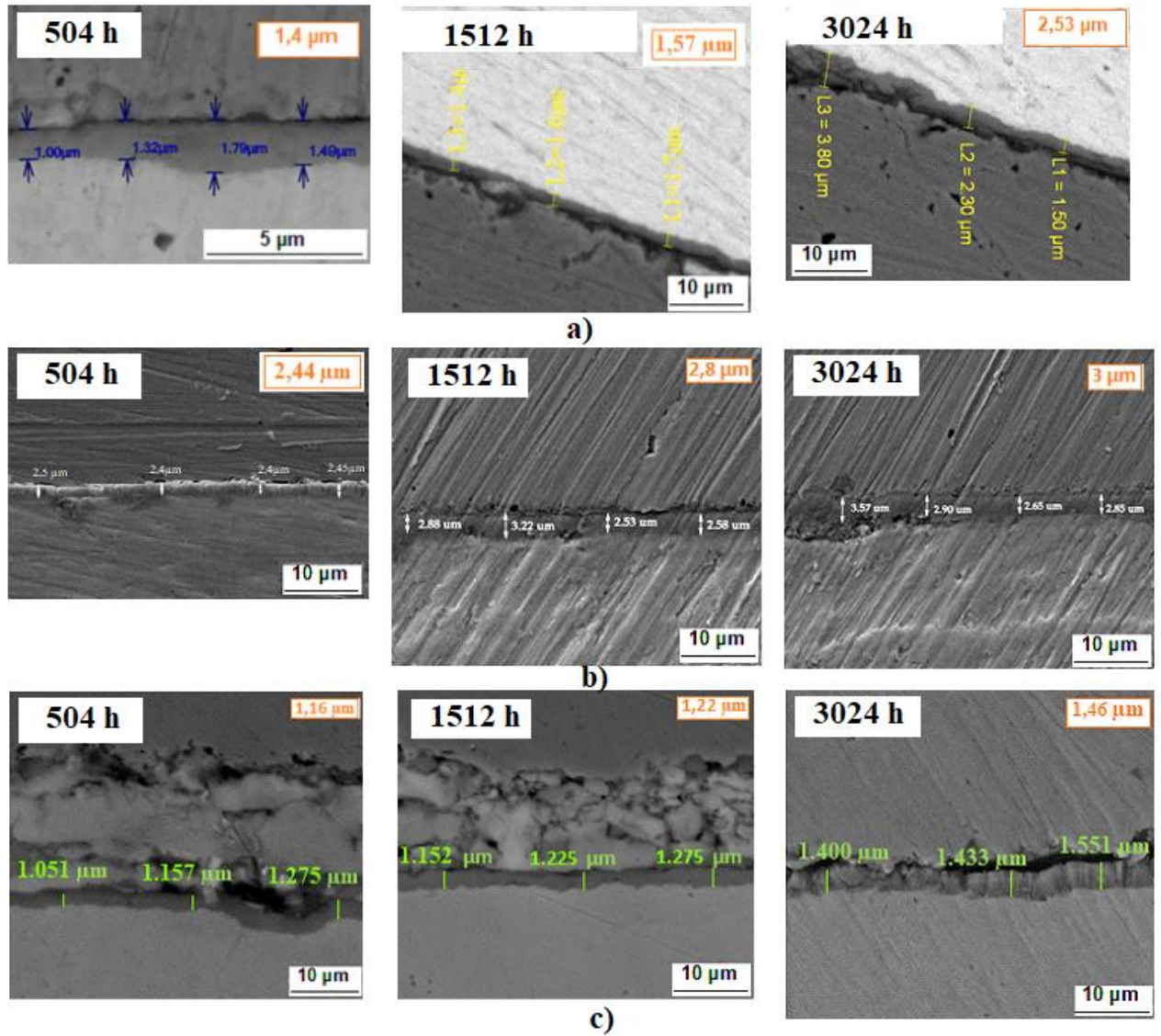
Fig. 3.23. The SEM cross-section micrographs for autoclaved Cr coated Zy-4 alloy after different autoclaving periods

As can be seen in these micrographs, all coatings maintained their integrity until the final of the autoclaving process. For Zy-4 samples coated by TVA and MS methods and tested for 3024 h, there were identified some areas that indicate a slight degradation of the coatings (the areas outlined with a white borders). However, as electrochemical results demonstrated, no decrease in the anticorrosive performances was observed in the chosen test environment, after 3024 h. Thus, we can consider that after 3024 h of autoclaving a critical point was achieved.

The results of SEM measurements are in good correlation with the results of gravimetric measurements, both showing an increase in layer thickness with autoclaving time.

Next, the the EDS line scan results for Zy-4 samples deposited with Cr and autoclaved for various periods of time are presented.

Set I - Zy-4/ Cr_TVA Samples

EDS line scan results for the Zy-4samples coated with Cr by TVA method are presented in Fig. 3.24. After the first two autoclaving cycles, chromium is identified in higher concentration, compared to O and Zr. Based on these data, an accelerated decrease of chromium can be observed at the end of the autoclaving process, with a value below the oxygen.
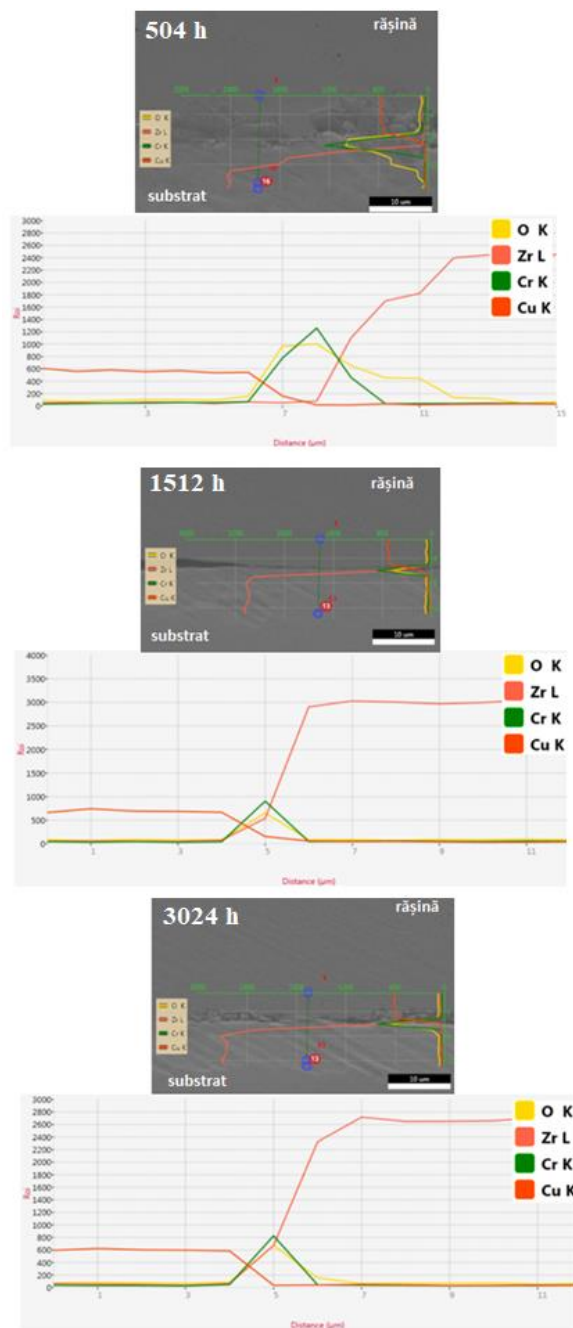
Fig. 3.24. EDS line scan analysis of Cr layer deposited on Zy-4 substrate by TVA method, after various periods of autoclaving

Set II - Zy-4/Cr_EBPVD samples

In the case of the samples deposited by EBPVD method, the results highlight the fact that there are no considerable variations of the elements of interest, Cr, O and Zr, in the area corresponding to the coating, Fig. 3.25. It is observed that for all three autoclaving periods the same ratio of elements is kept, chromium being found in the highest concentration. Oxygen shows a slightly downward trend, and zirconium is found in very low concentration in the middle area of the layer, increasing slightly towards the interface with the substrate, respectively towards the outside of the coating from the opposite side to the substrate. These results are in agreement with those obtained following the investigation of the surface by EDS analysis.

Fig. 3.25. EDS line scan analysis of Cr coating deposited on Zy-4 substrate by EBPVD method, after various times of autoclaving

Set III - Zy-4/ Cr_MS Samples

The cross-section elements variation was investigated on the Cr-coated Zy-4 samples deposited by MS method, and the results are shown in Fig. 3.26.
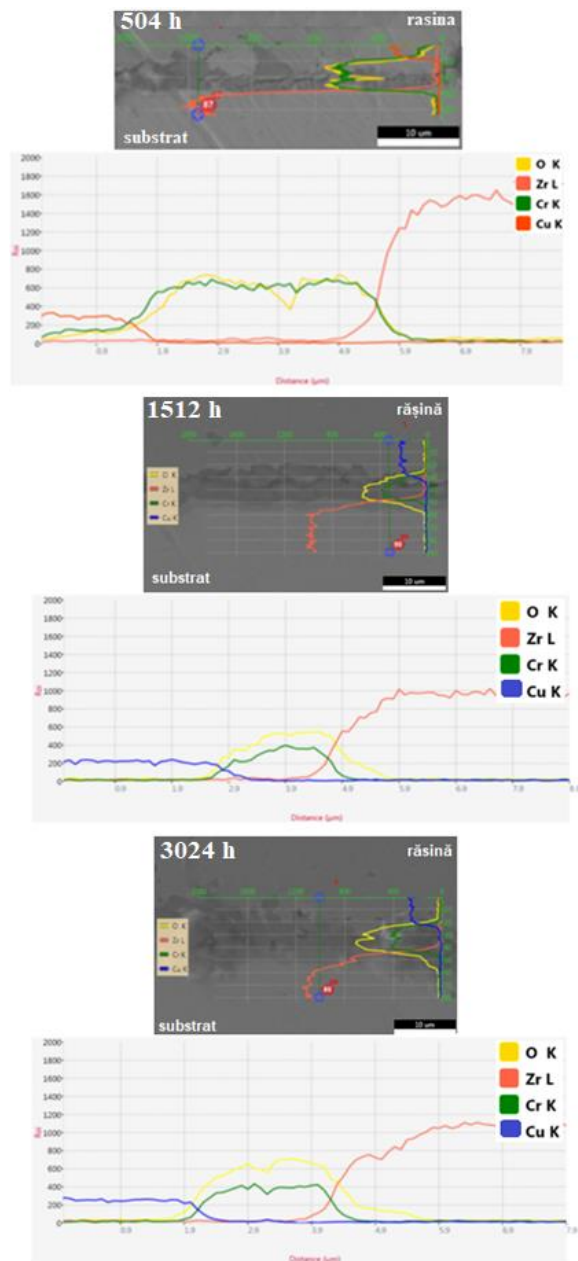
Fig. 3.26. EDS line scan analysis of Cr coating deposited on Zy-4 substrate by MS method, after various times of autoclaving

Following the spectra above, it is observed that after 504 h AC, in the investigated area related to the coating, chromium is found in a higher concentration than oxygen. In the case of both elements (Cr and O), the lack of fluctuations in the recorded concentrations was observed. For the next two test periods, the change in the ratio of recorded concentrations was identified, in favor of

increasing the concentration of oxygen compared to that of chromium, with the increase of the autoclaving period, which indicates the acceleration of the oxidation process from the coating - solution interface, under the test conditions.

3.2.4   Investigation of Cr coating by X-ray diffraction

Set I - Zy-4/ Cr_TVA Samples
In Fig. 3.27. the diffraction patterns obtained for Zy-4 samples coated with a chromium layer by TVA method are illustrated.
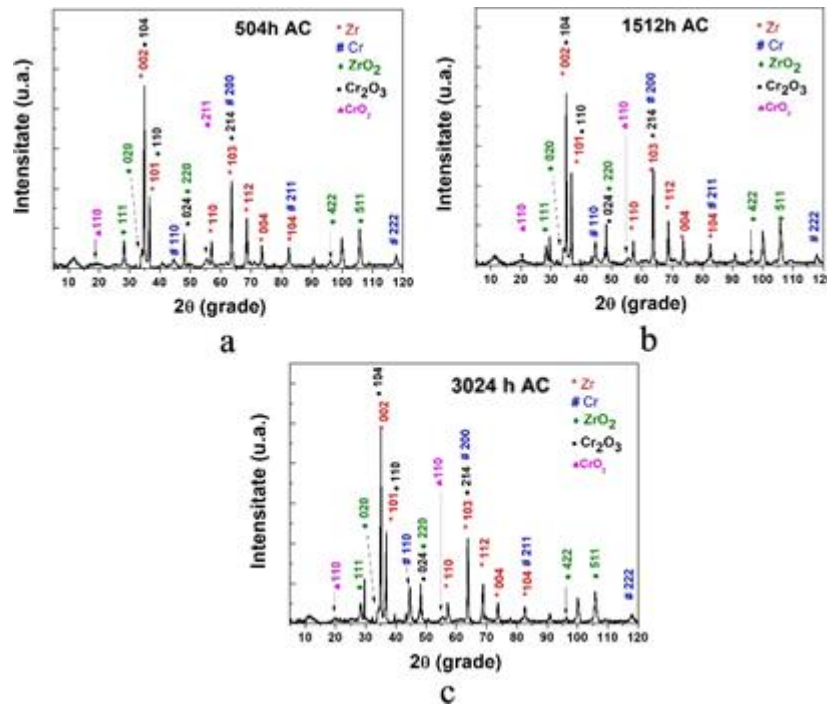
Fig. 3.27. The difractograms of Zy-4 samples deposited with Cr by TVA method and autoclaved various periods of time

Compared to the diffraction patterns resulting from the investigation of the uncoated Zy-4 samples [5], it can be observed the presence of an additional maximum around the value of 44.8 º. This peak was identified by comparison of the diffraction peaks with the corresponding structure sheets in the Crystal Open Database, as well as by verification in the Pearson Crystal Database, as belonging to a metallic phase of Cr, space group Im-3m (229) , with a volume-centered cubic arrangement in the unit cell and preferential crystallite growth along the (110) direction, similar to standard structure files. Along with the increase in autoclaving time, the intensity of the signals characteristic of chromium and zirconium is observed to decrease, while for zirconium oxide, an enhancement of the corresponding signal is recorded.

Set II - Zy-4/Cr_EBPVD samples
The diffractograms for the Zy-4 samples deposited with a Cr layer by EBPVD method are presented in Fig. 3.28.

Fig. 3.28. The difractograms of Zy-4 samples deposited with Cr by EBPVD method and autoclaved various periods of time

Unlike the samples covered by TVA, the coatings applied by EBPVD show a high degree of crystallinity of the layers. Also, in this case, the intensity of the maximum specific to chromium is higher than that of zirconium. This high degree of crystallinity obtained can be due either to a stoichiometric transfer of the material from the source to the substrate, but most likely due to a much higher thickness of the films deposited by EBPVD, compared to those applied by TVA.

The most widespread crystalline phase corresponds to the main element of the substrate, namely Zr, space group P63/mmc (194) with a hexagonal arrangement of atoms in the crystal lattice. The main hkl planes associated with the zirconium phase are (101), (102), (110), (103), (004), (112), (104) and the main preferential crystal growth along the (102) plane with the peak centered at 35 °. To avoid overloading the graphs shown in Fig., only the first three most intense reflection planes of zirconium are shown. The Cr layer deposited by the EBPVD method shows a high degree of crystallinity, highlighted by the peak centered at 44.5°. This peak is attributed to the (110) crystal plane of the metallic phase of chromium, space group Im-3m with a centered cubic crystal structure. The diffraction peaks observed at 35 °, 36.3 ° and 63.8 ° were attributed to Cr_2O_3, the main hkl planes associated being (104), (110) and (214). It is observed that the intensity of this maximum of Cr remains similar to the reference both for 504 h and for 1512 h, thus suggesting a good stability of the coating over time, under the autoclaving conditions, a decrease being observed at 3024 h. These observations are in good correlation with the results obtained by SEM/EDS investigations, where a stability of the coating was also observed during the autoclaving time.

In addition to these peaks specific to the various reflection planes specific to Zr and Cr, another peak can be observed at ~28°. Correlation of this peak with a crystalline phase was very difficult due to the lack of other specific additional orientations and due to the high intensity of the peaks corresponding to Zr and Cr. But, comparing with other similar data presented in the

specialized literature, this peak corresponding to the reflection plane (-111) of the monoclinic phase of ZrO_2 was identified.

Set III - Zy-4/ Cr_MS samples –

As for the previous two types of coatings, the structure of the Cr coatings deposited by MS method was also investigated by X-ray diffraction.

In Fig. 3.29. are presented the difractograms recorded for Cr coated Zy-4 samples by MS method.

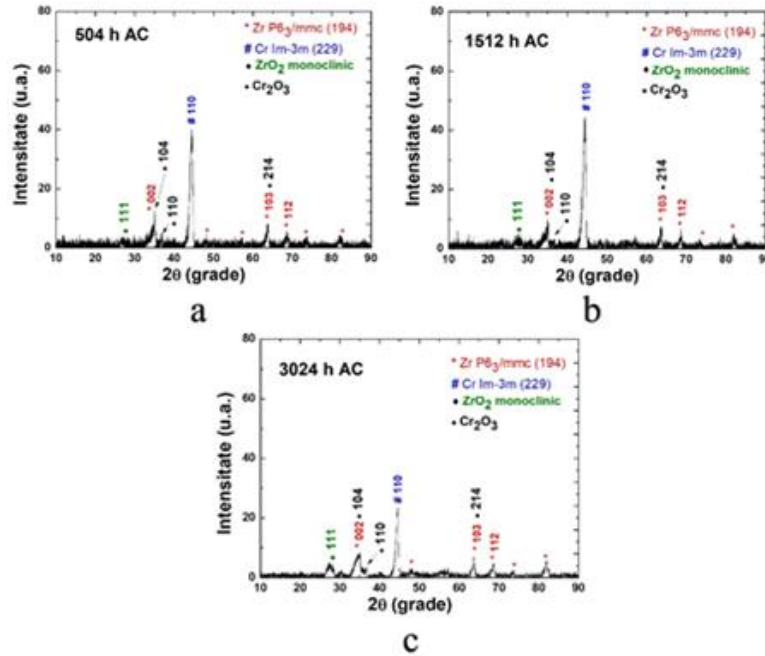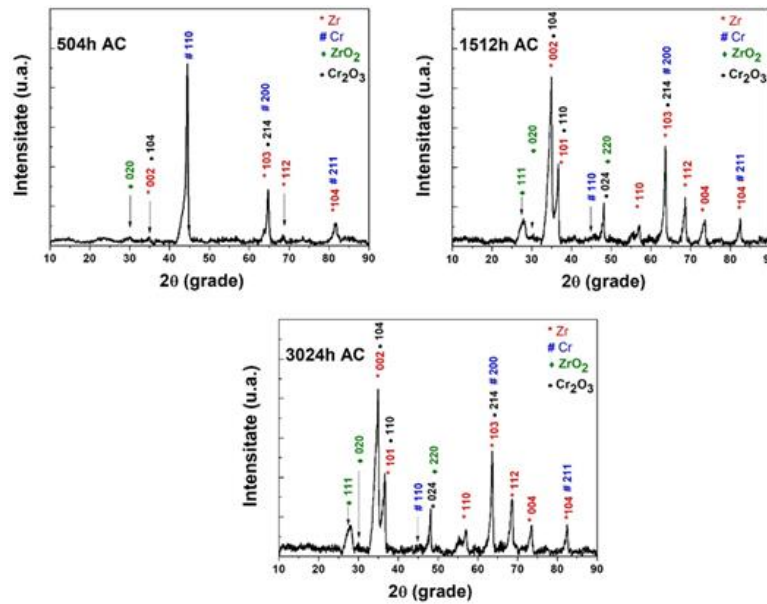Fig. 3.29. The difractograms of Zy-4 samples deposited with Cr by MS method and autoclaved various periods of time

The polycrystalline nature of the samples is clearly highlighted by the abundance of peaks corresponding to a biphasic crystal structure. These correspond to hexagonal zirconium P63/mmc (194), respectively the crystalline phase of monoclinic zirconium oxide. The last one being also identified in the case of Zy-4 samples deposited with Cr by the EBPVD method. Compared to the Zy-4/Cr_EBPVD samples, where the increase of the peak corresponding to the crystalline phase of ZrO_2 with the increase of the autoclaving time was observed, in this case this dependence is not identified. It was observed that the intensity of the ZrO_2 peak is higher after 504 h AC in the case of these samples, compared to the previously analyzed samples, but remains constant during the autoclaving process

3.2.5   XPS surface analysis

Overlaid XPS spectra of Cr, Zr and O are presented in Fig. 3.30., and in table 3.7. are summarized the relative concentrations of these elements. The XPS analysis was performed only for Zy-4/Cr_EBPVD samples.
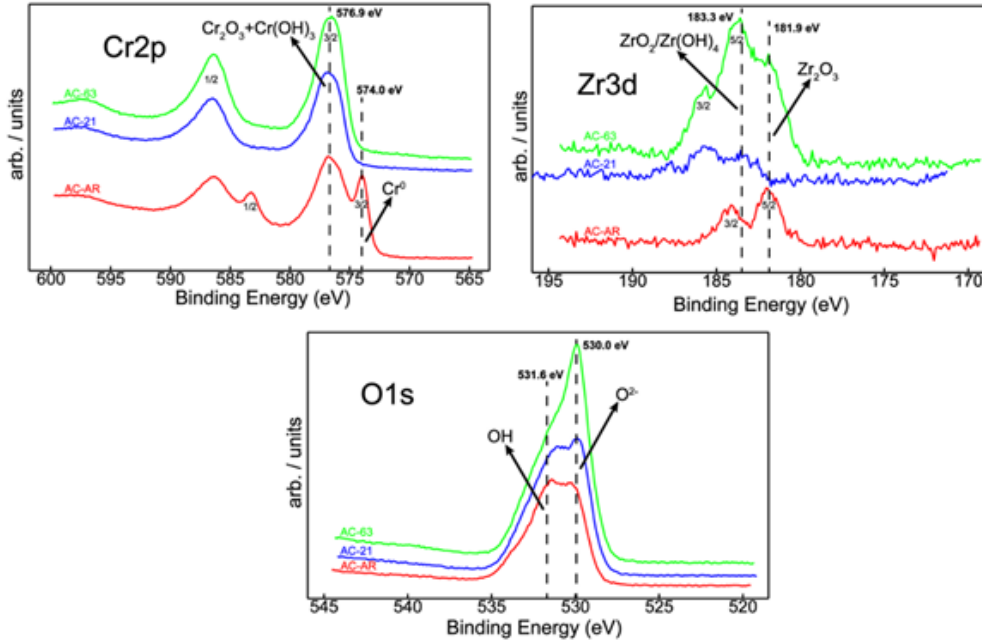
Fig. 3.4. Cr2p, Zr3d and O1s overlaid spectra, after various time of autoclaving

Tabel 3.7 Element relative concentrations (at. %)

AC time, h	C1s	N1s	O1s	Cr2p	Zr3d	O/Cr
0	44,0	3,7	36,1	16,0	0,2	2,3
504	46,6	3,5	40,1	9,7	0,1	4,1
1512	39,0	2,8	45,4	12,3	0,5	3,7

From Fig. 3.30. can be seen a different element evolution with autoclaving time.
In order to establish the chemical states of the elements, the spectra were deconvoluted into component peaks, as is presented in Fig. 3.31.
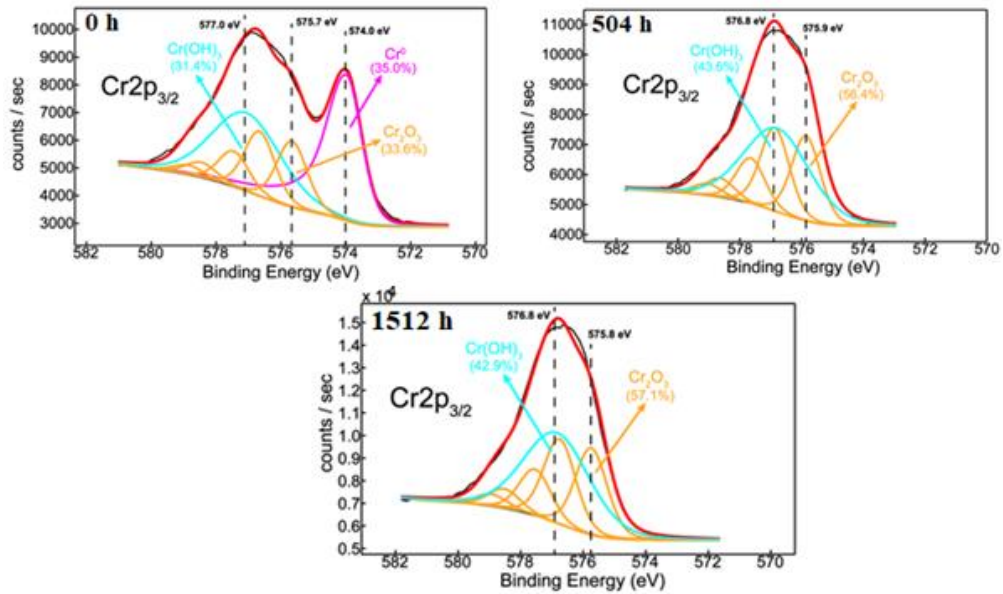
Fig. 3.5 Cr2p3/2 XPS deconvoluted spectrum for Zy-4/Cr_EBPVD after various time of autoclaving

It is observed, Fig. 3.31., that at the end of the autoclaving process the oxidized chromium concentration increases and metalic chromim was completely transformed.

Before autoclaving the chromium chemistry presents a mixture of equal concentrations of metalic chromium and oxidized chromium, table 3.8.

Table 3.8 Surface chemistry of chromium: chemical states and their relative concentrations

AC time, h	Binding energy [eV]	Cr chemical species	Cr relative concentrations [%]
0	574,0	$Cr^{metalic}$	35,0
	575,7	Cr_2O_3	33,6
	577,0	$Cr(OH)_3$	31,4
504	575,9	Cr_2O_3	56,4
	576,8	$Cr(OH)_3$	43,6
1512	575,8	Cr_2O_3	57,1
	576,8	$Cr(OH)_3$	42,9

3.2.6 Corrosion susceptibility evaluation by electrochemical methods

The applied electrochemical methods aimed the evaluation of the anticorrosive performance and the protective character of the Cr coatings applied on Zy-4 substrate, under high temperature and pressure conditions. The experiments were carried out under the same conditions to those specified in the previous chapter, for each individual electrochemical investigation.

3.2.6.1 Determination of the characteristics of oxide films formed after different autoclaving periods (EIS)

A qualitative evaluation of the protective character of the coatings was assessed by electrochemical impedance spectroscopy method.

Set I - Zy-4/ Cr_TVA samples

The Nyquist and Bode plots from Fig. 3.32. present the spectra recorded in open circuit, after 10 minutes of immersion in the test solution, for the Zy -4 samples coated by TVA method.

Fig. 3.32. Nyquist (a) and Bode (b) diagrams for Cr – TVA coated Zy-4 alloy, after differently autoclaving periods in the LiOH solution at 310°C and 10 MPa

The Niquist diagrams (Fig. 3.32. a) reveal a single open capacitive semicircle for non-autoclaved sample (0 h) and two capacitive semicircles for the autoclaved samples. In comparison to the non-autoclaved Cr-EBPVD-coated Zy-4 alloy, larger values of the capacitive semicircle diameter were obtained for all autoclaved samples. Compared with the non-autoclaved sample, larger values of the capacitive semicircle diameter were obtained for all autoclaved samples. We can see from the Bode plots (Fig. 3.32. b) that greater impedance values were observed for all Cr coated Zy-4 samples that were subjected to autoclaving for different periods. Since impedance is closely correlated with oxidizing resistance, we can conclude that these coatings have good corrosion resistance. The Bode diagram (Fig. 3.32. b) shows that two maxima of the phase angle are obtained, one at high frequencies and the other at low frequencies. The electrical equivalent circuit model shown in Fig. 3.33 was used to fit all experimental data measured by electrochemical impedance spectroscopy method.
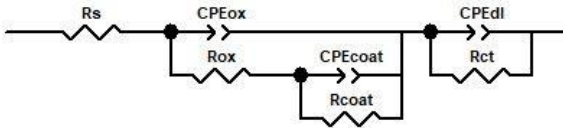
Fig. 3.33. The electric equivalent circuit proposed for Cr-TVA-coated Zy-4 samples, after different autoclaving periods

The elements of the equivalent circuit are described as follow:

- R_s – solution resistance between the electrode and the electrolyte;
- CPE_{ox} – constant phase element of the oxide layer;
- R_{ox} – resistance of the oxide layer;
- CPE_{coat} – constant phase element of the coating;
- R_{coat} – resistance of the coating;
- CPE_{dl} – constant phase element for double layer;
- R_{ct} – resistance to charge transfer.

It is noteworthy that constant phase elements (CPE) must be introduced to explain the deviation of the capacitances between the actual measurements and the ideal pure capacitances, due to the local inhomogeneities of the dielectric material, surface roughness and the relaxation effect, and the degree of deviation from the ideal capacitance depends on the value of $n(0 < n < 1)$. A good fit of the data to this model was obtained and the fitting parameters are listed in table 3.9.

Table 3.9. The values of equivalent electrical circuit elements for as-coated Cr Zy-4 alloy and autoclaved Cr coated Zy-4 alloy by TVA method

AC period, h	R_s, $K\Omega \times cm^2$	CPE_{ox}-T $nF \times cm^{-2}$	CPE_{ox}-P	R_{ox} $K\Omega \times cm^2$	CPE_{coat}-T $\mu F \times cm^{-2}$	CPE_{coat}-P	R_{coat} $\Omega \times cm^2$	CPE_{dl}-T $\mu F \times cm^{-2}$	CPE_{dl}-P	R_{ct} $\Omega \times cm^2$	Chi-Squared
0	15,85	-	-	-	1,51	0,89	$8,62 \times 10^5$	1,97	0,76	26974	$2,7 \times 10^{-3}$
504	15,87	0,161	0,98	1,25	1,93	0,63	$1,97 \times 10^5$	1,81	0,94	$2,89 \times 10^7$	$4,1 \times 10^{-3}$
1512	14,32	1,35	0,93	57,97	1,21	0,79	$1,81 \times 10^6$	0,122	0,98	$3,82 \times 10^{10}$	$1,1 \times 10^{-3}$
3024	15,23	3,56	0,88	16,06	0,94	0,78	$5,6 \times 10^6$	0,295	0,79	$4,9 \times 10^{10}$	$1,8 \times 10^{-3}$

Based on the above table we observe that R_{coat} increases and CPE_{coat} decreases with autoclaving time, so it can be stated that the coating and oxides formed after autoclaving have a high resistance to electrolyte diffusion through the pores of the coating and oxides, a slight decrease of this property being observed after 3024 h of autoclaving.

It can also be seen that R_{ct} shows much higher values for the autoclaved samples compared to the as-coated sample, which indicates a higher resistance in the corrosion reaction. The highest value obtained was for the sample autoclaved for 1512 h.

CPE_{dl} represent the wetted surface under the coating [12]. Thus, as CPE_{dl} value is lower, a smaller surface has been exposed to the electrolyte. In the the present case, a decrease of CPE_{dl} can be observed with increasing of autoclaving time, which indicate that the coating and the oxides act as an efficient diffusion barrier.

Set II - Zy-4/Cr_EBPVD samples

The Nyquist and Bode plots from Fig. 3.34. present the spectra recorded in open circuit, after 10 minutes of immersion in the test solution, for the Zy -4 samples coated by EBPVD method.
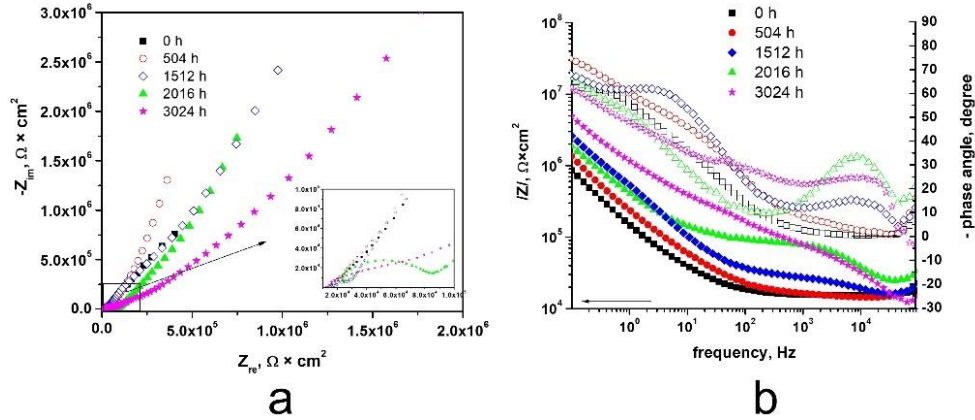
Fig. 3.34. Nyquist (a) and Bode (b) diagrams for Cr – EBPVD coated Zy-4 alloy, after differently autoclaving periods in the LiOH solution at 310°C and 10 MPa

Based on the Niquist diagram (Fig. 3.34. a), it is observed, as for previous samples, a single capacitive semicircle, and in the case of the autoclaved samples, the formation of two capacitive semicircles was observed, in accordance with the generated interfaces. Compared to the as-coated sample, larger capacitive semicircle diameters were obtained for the autoclaved samples.

Following the Nyquist diagram (Fig. 3.34. b) it can be seen in the low frequency domain that the impedance value is higher for samples autoclaved for longer times. Taking into account the fact that the impedance at low frequency values is related to the Faradaic process [12], [13], we can say that the protective properties of the film increased with the autoclaving time.

Based on the Bode diagrams (Fig. 3.34. b), high impedance values were determined for all autoclaved samples for distinct periods of time, which demonstrates a higher resistance to corrosion compared to the as-coated sample.

The equivalent circuit model used to fit the experimental EIS data is shown in Fig. 3.35.
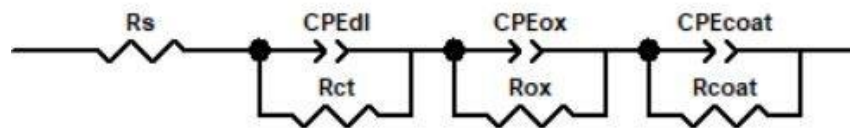
Fig.3.35. The electric equivalent circuit proposed for Cr-TVA-coated Zy-4 samples, after different autoclaving periods

The equivalent electrical circuit elements are described in the section of samples deposited by TVA.

The data summarized in table 3.10. show a very good fitting of the experimental data with this equivalent circuit model.

Table 3.10. The values of equivalent electrical circuit elements for as-coated Cr Zy-4 alloy and autoclaved Cr coated Zy-4 alloy by EBPVD method

AC time, h	R_s, $\Omega \times cm^2$	CPE_{dl}-T $\mu F \times cm^{-2}$	CPE_{dl}-P	R_{ct} $M\Omega \times cm^2$	CPE_{ox}-T $nF \times cm^{-2}$	CPE_{ox}-P	R_{ox} $\Omega \times cm^2$	CPE_{coat}-T $\mu F \times cm^{-2}$	CPE_{coat} -P	R_{coat} $M\Omega \times cm^2$	Chi-Squared
0	200.9	0.18	0.87	2.18	-	-	-	0.15	0.80	648	3.3×10^{-4}
504	143.5	1.22	0.75	0.46	30.45	0.88	9167	0.99	0.74	2.06×10^{10}	4.9×10^{-5}
1512	149.3	1.18	0.85	0.45	10.15	0.91	8597	0.95	0.78	5.81×10^{10}	1.1×10^{-5}
3024	154.4	1.23	0.76	0.58	12.89	0.93	8308	0.98	0.88	1.17×10^{11}	4.3×10^{-5}

The resistance of the coating and the resistance of the solution from the pores of the coating are in correlation [12]. From the above table, we observe that R_{coat} increases with autoclaving time, which means that the oxides formed on the surface of coating has high resistance to electrolyte diffusion.

High values of CPE_{coat}-P, CPE_{ox}-P, CPE_{dl}-P are calculated, which demonstrate that both Cr coating and the oxides are protecting the substrate [14].

From the table above we identify the highest value of R_{ct} corresponding to as-coated Zy-4 sample. The autoclaved samples present closed R_{ct} values, the higher corresponding to the sample autoclaved for 3024 h.

As R_{coat} presents higher values than R_{ct}, we deduce that R_{coat} has the main influence on the corrosion behaviour of coated Zy-4 alloy.

We also notice the growth of coating resistance with autoclaving time, wich demonstrate the anticorrosion protection of the Zy-4 alloy due to the chromium coating.

The values of constant phase elements are close to 1, demonstrating a capacitive character of the coating.

Set III - Zy-4/ Cr_MS Samples

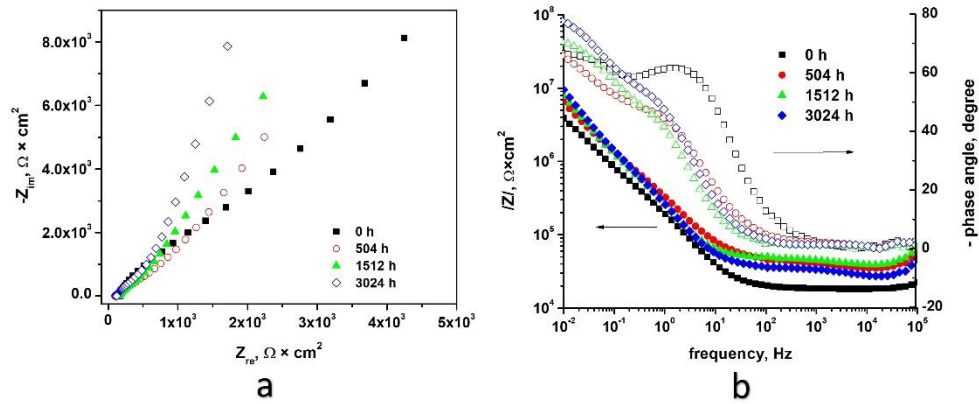The Nyquist and Bode plots for Zy-4/Cr_MS are presented in Fig. 3.36.
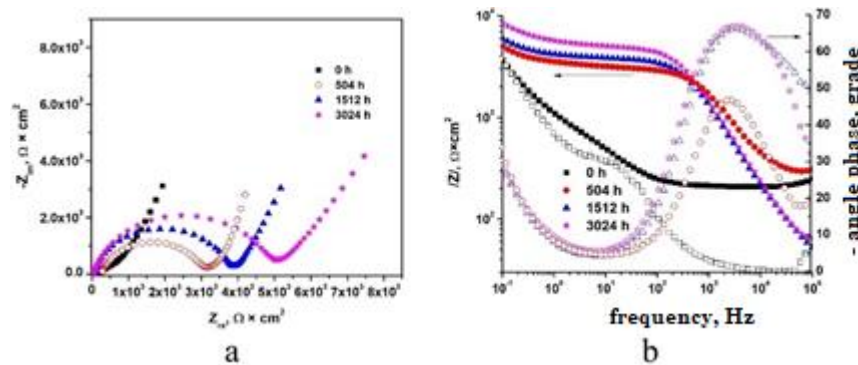

Fig. 3.6 Nyquist (a) and Bode (b) diagrams for Cr – MS coated Zy-4 alloy, after differently autoclaving periods in the LiOH solution at 310°C and 10 MPa

As can be seen from above figure, the autoclaved Zy-4/Cr samples presents higher impedance values than those corresponding to non-autoclaved Zy-4/Cr samples. Closed values for

impedance have been observed, the highest corresponding to the sample autoclaved for 3024 h. These results confirm the presence of an outer layer with high protective properties during the entire autoclaving process.

The equivalent circuit model used to fit the experimental EIS data is shown in Fig. 3.37.
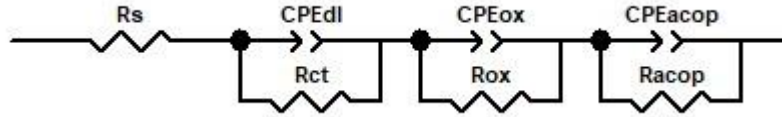
Fig. 3.7 The electric equivalent circuit proposed for Cr-MS-coated Zy-4 samples, after different autoclaving periods

As for previous case, the equivalent electrical circuit elements are described in the section of samples deposited by TVA.

The data summarized in table 3.11 show a very good fitting of the experimental data with this equivalent circuit model.

Table 3.11 The values of equivalent electrical circuit elements for as-coated Cr Zy-4 alloy and autoclaved Cr coated Zy-4 alloy by MS method

AC time, h	R_s, $\Omega \times cm^2$	CPE_{dl}-T $\mu F \times cm^{-2}$	CPE_{dl}-P	R_{ct} $M\Omega \times cm^2$	CPE_{ox}-T $nF \times cm^{-2}$	CPE_{ox}-P	R_{ox} $\Omega \times cm^2$	CPE_{coat}-T $\mu F \times cm^{-2}$	CPE_{coat}-P	R_{coat} $M\Omega \times cm^2$	Chi-Squared
0	20,2	$3,7\times10^{-4}$	0,64	$1,8\times10^{14}$	-	-	-	$7,1\times10^{-6}$	0,79	201,2	$2,3\times10^{-3}$
504	17,3	$3,2\times10^{-7}$	0,84	2881	$4,6\times10^{-4}$	0,71	$1,9\times10^{14}$	$7,8\times10^{-6}$	0,99	267,1	1.3×10^{-3}
1512	18,7	$2,6\times10^{-7}$	0,89	3723	$4,1\times10^{-4}$	0,78	$7,5\times10^{18}$	$4,2\times10^{-5}$	0,87	109,1	2.5×10^{-4}
3024	19,3	$2,7\times10^{-7}$	0,87	4920	$2,7\times10^{-4}$	0,64	$7,8\times10^{19}$	$1,1\times10^{-4}$	0,69	57,6	3×10^{-4}

The highest value of R_{coat} correspond to the sample autoclaved for 504 h and it is showing a decreasing behaviour as autoclaving time increases.

3.2.6.2 Open Circuit Corrosion Potential Measurements

The generalized corrosion behaviour prediction of coated Zy-4 alloy was studied by applying open circuit potential measurements. The tests have been carried out at room temperature in simulating primary chemistry solution of CANDU reactor. The results are presented as diagrams Ecorr vsTime.

Set I - Samples of Zy-4/ Cr_TVA

In Fig. 3.38. is presented the open circuit potential variation for Zy-4/ Cr_TVA samples, autoclaved differently periods of time, recording a relative stable evolution for all the tested samples. It is also noted that there were not recorded higher potential variations, which could indicate possible discontinuities of coating.
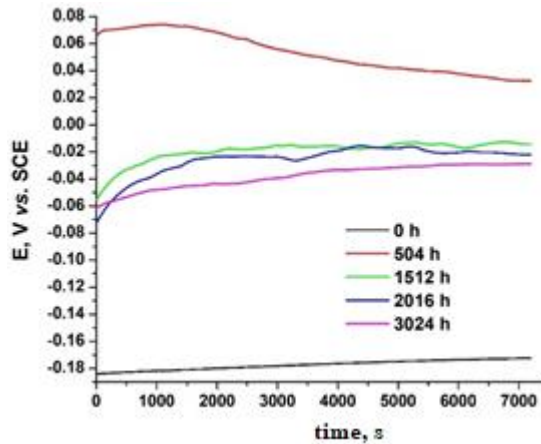
Fig. 3.38. Open circuit potential variation for Zy-4/ Cr_TVA samples, autoclaved various periods of time

In table 3.12. are summarized the initial and stabilized values of the corrosion potential for the evaluated samples.

Table 3.12. Corrosion potential values for Zy-4/ Cr_TVA samples

AC time, h	0	504	1512	2016	3024
Initial Ecorr, mV	-182	66	-55	-72	-62
Stabilized Ecorr, mV	-172	32	-14	-22	-28

Following the recorded data, it can be observed that for the as-coated Zy-4/Cr sample (0 h) was get the most electronegative value of Ecorr (-172 mV). The sample tested 504 h started from the most electropositive value of the OCP (66 mV), leveled to a lower value of Ecorr (about 30 mV), which indicate a slow corrosion potential decrease. Samples tested longer periods have started from a corrosion potential in the cathodic zone (-55 ÷ -72 mV), presenting a slight increase up to the stabilization value (-14 ÷ - 28 mV).

Set II - Zy-4/Cr_EBPVD samples
The trend of corrosion potentials for the Zy-4 samples coated with Cr by EBPVD method and autoclaved for different periods of time are shown in Fig. 3.39.
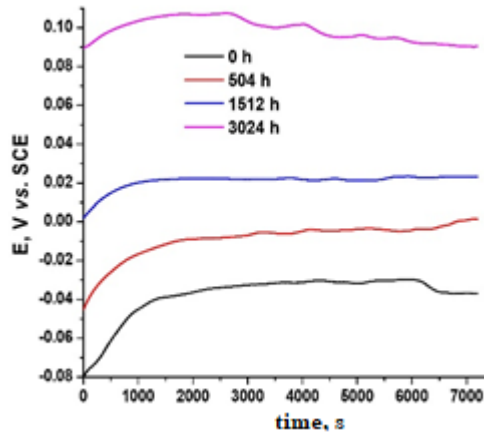
Fig. 3.39. Open circuit potential variation for Zy-4/ Cr_EBPVD samples, autoclaved various periods of time

As can be notice from the figure above, small fluctuations in the evolution of the corrosion potential were recorded during the test time. The non-autoclaved Cr-EBPVD-coated Zy-4 sample (0 h) showed a high rate of increase in Ecorr, after 1400 s increasing from −80 mV to −39 mV, followed by a plateau for about 6500 s, after which a slight decrease and leveling was observed, table 3.13. The samples autoclaved 504 h and 1512 h, respectively, showed very close evolutions of the corrosion potentials for the first 2500 s. After this point, a shift in the curves was observed, the sample autoclaved 1512 h, moved towards more electropositive values of Ecorr, compared to the sample autoclaved 504 h. The sample autoclaved at 3024 h showed a different behavior, the corrosion potential starting from the highest values (89 mV) compared to the other samples (which had Ecorr in the cathodic range), but after approximately 2700 s, the potential of corrosion registered a continuous downward trend.

Table. 3.13. Corrosion potential values for Zy-4/ Cr_EBPVD samples

AC time, h	0	504	1512	3024
Initial Ecorr, mV	-80	- 41	- 39	89
Stabilized Ecorr, mV	-39	- 9	5	22

Set III - Zy-4/ Cr_MS Samples

The Ecorr evolution has been recorded for 7200 s and it is presented in Fig. 3.40.
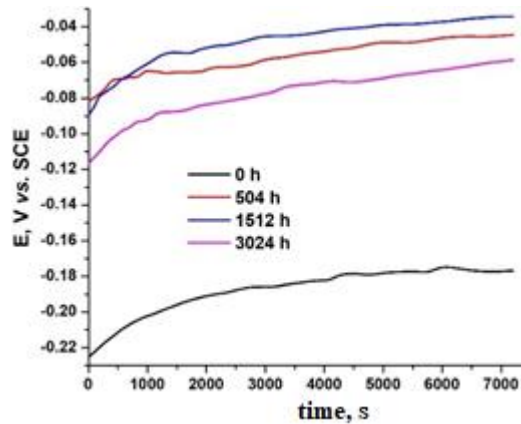
Fig. 3.40 Open circuit potential variation for Zy-4/ Cr_MS samples, autoclaved various periods of time

Compared to the samples coated by TVA and EBPVD, where it was observed a very quick stabilizitation of the Ecorr after the begining of the test, in this case it was seen an increasing Ecorr trend up to the final of the test. An decay about 100 mV can be observed between the non-autoclaved sample and the autoclaved samples. Thus can suggest the protective role of chromium oxide[11], [3], [24], [25] developed during the autoclaving process. The sample autoclaved for 1512 h presented Ecorr values closer to anodic domain, while the sample autoclaved for 3024 h showed a decay about 40 mV towards cathodic domain.

In table 3.14. are presented the initial and final Ecorr values for the Zy-4/Cr_MS samples.

Table 3.14 Corrosion potential values for Zy-4/ Cr_MS samples

AC time, h	0	504	1512	3024
Initial Ecorr, mV	-225	-80	-90	-115
Final Ecorr, mV	-180	-48	-37	-62

Because of the continuous Ecorr trend, the stabilized Ecorr was replaced by the final Ecorr. This trend confirm the formation of a passive layer which confer corrosion protection.

3.2.6.3 Potentiodynamic linear polarization method

Set I - Zy-4/ Cr_TVA samples

In order to see the Cr coated Zy-4 alloy corrosion behavior in a specific primary circuit solution (LiOH solution, pH 10.5), the potentiodynamic polarization curves of for sample before and after different autoclaving period were recorded and are illustrated in Fig. 3.41.
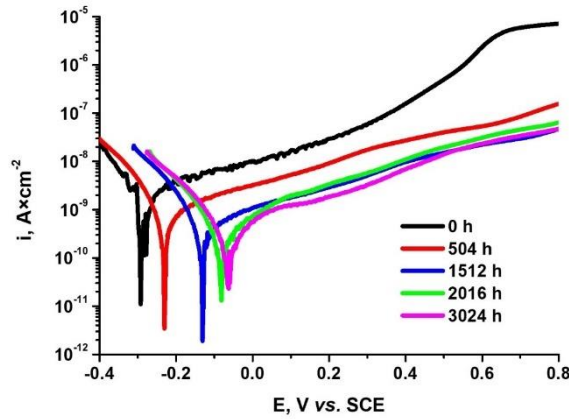
Fig. 3.41. Potentiodynamic polarization curves for Zy-4/ Cr_TVA samples

As can be seen from the above figure, the as-coated Zy-4/Cr sample presents more electronegative values of Ecorr and higher corrosion currents compared to the Zy-4/Cr autoclaved samples. Also, it can be notice that the Zy-4/Cr samples autoclaved for 2016 and 3024 h respectively, showed a very closed electrochemical behaviour.

The electrochemical parameters resulted from polarization tests are presented in table 3.15.

Table 3.15. Polarization parameters of Zy-4/Cr_TVA samples autoclaved for different periods in LiOH solution (310 °C, 10 MPa)

AC time, h	Tafel Slope Method				Polarization Resistance Method		E, %	P (%)
	E_{cor}, mV	i_{cor}, nA×cm^{-2}	Kg, µg×m^{-2}h^{-1}	P, nm×an^{-1}	R_P, MΩ	i_{cor}, nA×cm^{-2}		
0	−283	1,192	20,47	27,32	7,7	2,27	−	-
504	−225	0,492	8,46	11,29	52	0,403	58,65	0,023
1512	−119	0,147	2,52	3,37	140	0,143	87,65	$2,9× 10^{-4}$
2016	-74	0,107	1,84	2,45	190	0,101	91,01	$0,51× 10^{-4}$
3024	−59	0,098	1,68	2,25	250	0,119	91,76	$0,22× 10^{-4}$

For coating corrosion evaluation an important factor is the protection efficiency (P), which allows the assessment of coating integrity. As can be seen in the above tabel, the autoclaved sample present higher values of P. Also, lower values of corrosion rates and current densities have been obtained, compared to uncoated Zy-4 samples and autoclaved in the same conditions [15].

It was also determined that the Zy-4/Cr sample autoclaved for 3024 h presented the best corrosion protection. For this sample the oxide layer presents the smallest porosity value as well as the smallest current density.

Set II - Zy-4/Cr_EBPVD samples

The potentiodynamic curves recorded in LiOH electrolyte, at 10.5 pH and room temperature (22 ± 2 °C), for the Cr-EBPVD-coated Zy-4 samples and autoclaved for different periods under primary

circuit conditions of the CANDU nuclear reactor are shown in Fig. 3.42. Based on these, a decrease in the corrosion current density can be observed simultaneously with the movement toward more electropositive values of the corrosion potential values along with the increase in the autoclaving time for all studied samples.
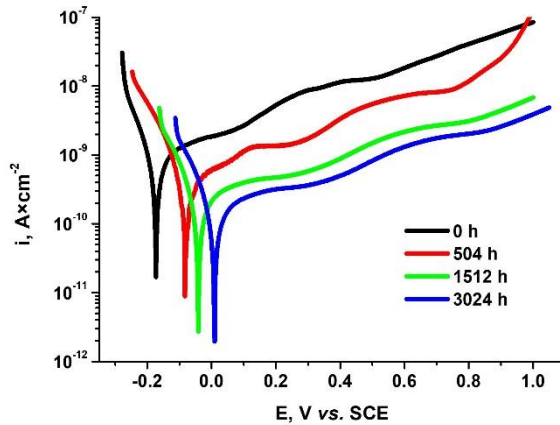
Fig. 3.12. Potentiodynamic polarization curves for Zy-4/Cr_EBPVD samples

The values of the electrochemical parameters determined by potentiodynamic polarization tests on the Cr-EBPVD-coated Zy-4 samples are included in table 3.16. Also, applying relations (1) and (2), the two factors used in evaluating the integrity of a coating, the porosity coefficient, and the protection efficiency, were calculated.

Table 3.16. Polarization parameters of Zy-4/Cr_EBPVD samples autoclaved for different periods in LiOH solution (310 °C, 10 MPa)

AC time, h	E_{cor}, mV	Tafel Slope Method				Polarization Resistance Method		E, %	P (%)
		i_{cor}, $nA \times cm^{-2}$	Kg, $\mu g \times m^{-2} h^{-1}$	P, $nm \times an^{-1}$	R_P, $M\Omega$	i_{cor}, $nA \times cm^{-2}$			
0	-167	0,586	10,08	13,45	48,1	0,543	–	-
504	-75	0,269	4,63	6,17	110	0,231	54,01	0,041
1512	-33	0,091	1,58	2,11	350	0,073	84,33	0,0045
3024	25	0,059	1,02	1,35	620	0,051	89,92	0,0007

According to the data in the above table, for the autoclaved samples, the values of the corrosion potentials, as well as the corrosion currents, are located towards more electropositive values, compared to the as-coated sample. It can also be observed that the values of the corrosion rates decreased with the autoclaving time. These data are corroborated by the values obtained for the porosity coefficient and the protection efficiency, which demonstrate the maintenance of the anticorrosive properties of the coating, as well as their strengthening.

Set III - Zy-4/ Cr_MS Samples

In Fig. 3.43. are presented the polarization curves for Zy-4/Cr_MS samples, autoclaved for various periods.
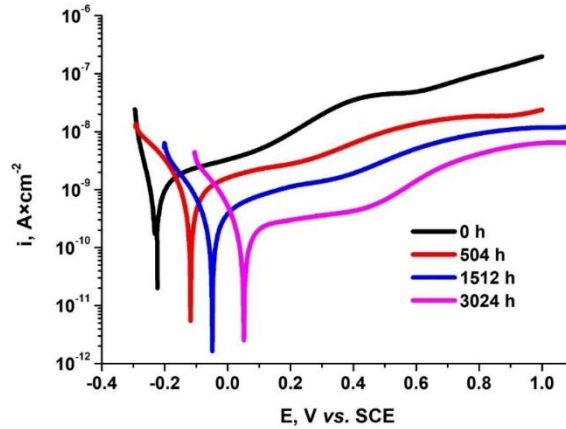
Fig. 3.43 Potentiodynamic polarization curves for Zy-4/Cr_EBPVD samples

Based on Fig. 3.43. it can be observed an almost constant decay, about 10 mV, between the recorded potentials, with a tendency to anodic domain as autoclaving time increase.

As for the previous samples, the electrochemical parameters have been determinated by Tafel and Polarization resistance methods, table 3.17.

Tabel 3.17 Polarization parameters of Zy-4/Cr_MS samples autoclaved for different periods in LiOH solution (310 °C, 10 MPa)

| Timp AC, h | E_{cor}, mV | Tafel Slope Method | | | Polarization Resistance Method | | E, % | P (%) |
		i_{cor}, nA×cm^{-2}	Kg, µg×m^{-2}h^{-1}	P, nm×an^{-1}	R_P, MΩ	i_{cor}, nA×cm^{-2}		
0	-232	0,797	13,71	18,3	31,2	0,787	–	-
504	-117	0,515	8,86	11,82	55,1	0,476	35,38	0,0166
1512	-54	0,216	3,72	4,96	210	0,229	72,89	$6,3× 10^{-4}$
3024	-56	0,121	2,08	2,77	375,0	0,122	84,82	$0,12× 10^{-4}$

The electrochemical parameters determinated by these two methods presents closed values, giving a high confidence in the obtained results. The values of corrosion currents are proportional with the corrosion rates, both decreasing as autoclaving time increases. Moreover, there were obtained high values of Rp (MΩ magnitude), which are increasing with autoclaving time increasing. The highest value was obtained for the sample autoclaved for 3024 h.

4 GENERAL CONCLUSIONS AND FUTURE RESEARCH DIRECTIONS

General conclusions

The thesis had provide an insight into corrosion process of chromium coated Zy-4 alloy in a CANDU primary circuit conditions environment.

Considering the experimental study and the analyzes applied in this doctoral study, the main conclusions will be presented below.

In the present work, a literature review was carried out into two research directions: use of zirconium alloys in the nuclear field and accident tolerant fuels development and testing, with the focus on the development and testing of metallic chromium coatings, deposited on zirconium alloy substrate.

An initial and post-autoclaved assessment of corrosion behaviour, as well as the morphological and structural properties have been carried out.

This doctoral study evaluates three types of chromium coatings, deposited by three physical deposition methods: TVA, EBPVD and MS.

In the first part of this work it was highlighted that all three types of coatings presented morphological and structural characteristics that recommend them for high temperature and pressure use. Also, the coated Zy-4 alloy presented improved corrosion performance.

Next to initial pre-characterization it was assesst the corrosion behaviour of coated Zy-4 alloy over a period up to 3024 h of autoclaving in CANDU primay circuit conditions.

Since the reduction of hydrogen absorption is a very important aspect that is desired to be mitigated by the deposition of such diffusion barrier layers, a qualitative evaluation of the appearance of zirconium hydrides was carried out. Acicular hydride precipitation was observed with a relative uniform distribution in a circumferential distribution.

Vickers microhardness evaluation revealed a low hardening of the material with the increasing of the autoclaving time. This can be explained as a result of the formation of zirconium hydrides, as well as due to the working conditions (temperature, pressure, test chemistry). Also, the highest value was obtained for the Zy-4 samples coated with Cr by EBPVD method, most likely due to the fact that in this case the substrate was preheated to a value of approx. 400 °C.

Gravimetric evaluation of the tested samples showed a lower mass gain for all Cr coated Zy-4 samples compared to the uncoated Zy-4 samples. It was also noticed that the corrosion rates decrease with the oxide layer growing. Thus it can be concluded that the transport of oxidising species through the oxide layer is controlling the corrosion rate. It was determined that corrosion kinetics follows a cubic law, with a very good confidence factor for all the tested samples ($R^2 \sim$ $0.993 \div 0.999$, depending on the deposition method applied).

During the corrosion testing process, a possible loss of the integrity of these coatings was investigated, but no areas indicating delamination or localized corrosion of the coatings were observed.

The thicknesses of the layers increase with the autoclaving time, being in good correlation with the gravimetric measurements. Values of layer thicknesses between $1 \div 3$ µm were measured.

The stability of the Cr layer is very important for maintaining anti-corrosion performance over a long period of time. Thus, the elemental distribution carried out on the surface of Zy-4 samples coated with Cr and tested for different periods of time shows a decrease in chromium concentration with autoclaving time. The Zy-4 samples coated with Cr by EBPVD method show the best stability of the coating, in the case of these samples minor variations in the concentration

of the elements of interest have been seen, while the Zy-4 samples coated with Cr by TVA method presented an accelerated downward trend of the elements of interest with autoclaving time.

Also, the EDS line scan analysis pointed out the decrease in the concentration of Cr with the increase of the autoclaving time, and the smallest variations of the elements Cr, O and Zr, in the area corresponding to the Cr layer, were recorded for the Zy-4 samples coated with Cr by EBPVD method.

The assessment of Cr coatings structure depending on the autoclaving time illustrated the dcrease of the intensity of the Cr and Zr signals, while ZrO_2 and Cr_2O_3 presented an increase in corresponding signals. Based on these, it was concluded that the samples coated with Cr by EBPVD method have shown the highest degree of crystallinity, also noting that in this case the intensity of the specific maximum of chromium is higher than that of zirconium, even after the last autoclaving period.

The XPS measurements were performed to obtain information about surface chemistry and the oxidation states of the detected elements. Thus it was observed a chemical behaviour depending on autoclaving time of Cr and Zr. Before autoclaving it was identified a mixture of equal concentrations of metalic chromium amd oxidezed chromium, but at the end of the process the ozidized chromium concentration increases and metalic chromium was completely transformed.

The anticorrosive performance of chromium coatings during the autoclaving process was also investigated by applying electrochemical methods.

The evaluation of the Cr coatings using electrochemical impedance spectroscopy revealed that the formation of very thin layers of chromium oxide (of the order of nanometers) on the surface of the Cr coatings increased the degree of protection offered to the Zy-4 substrates. Thus, it was identified that the obtained impedance and polarization resistance values increase with the increase of autoclaving time. Also, the values of constant phase elements are close to 1, which demonstrate that the coatings exhibit an capacitive behavior.

The use of corrosion potential variation method also allowed the investigation of the stability of the coating at the interface with the electrolyte. The corrosion potential was recorded over a time up to 7200 s. During this testing time, small fluctuations were recorded in the evolution of the corrosion potential for all three types of coatings, indicating their good continuity and stability over time.

The linear potentiodynamic polarization measurements led to obtaining the electrochemical parameters specific to the investigated corrosion process. Due to the protective properties of the thin layer of Cr_2O_3 it was observed an increase of anticorrosive performance with the increase of autoclaving time. A more protective behaviour of the Cr coating deposited by EBPVD was highlighted by the results obtained. Integrity evaluation of the coatings by determining the oxide porosity and protection efficiency parameters has indicated that the Cr coating developed by EBPVD method presented higher anticorrosive performance.

Future research directions

This research has thrown up a number of aspects that should be explored with further experimentation:

- Optimizing the working parameters characteristic to the physical deposition method, in order to obtain advanced chromium coatings;
- Evaluation of the anticorrosive properties of metallic chromium coatings by exposure in controlled environments for a longer period of time, minimum 200 days;

- Mechanical tests to evaluate the influence of the autoclaving conditions on the mechanical properties of the coated Zy-4 alloy;
- Performance evaluation of metallic chrome coating under LOCA accident conditions;
- Behaviour of the metallic chromium coatings under irradiation conditions;
- Water chemistry analysis to assess the posibility of mitigation of some species from coatings to testing solution. This evaluation is relevant both for coating integrity and the potential of coating to produce impurities and deposits;
- Quantitative evaluation of hydrogen uptake.

5 PERSONAL CONTRIBUTIONS AND SCIENTIFIC ACHIEVEMENTS IN THE FIELD OF DOCTORAL STUDY

PERSONAL CONTRIBUTIONS

Literature review of the most relevant studies on the topic of development, testing and characterization of the coatings for accident tolerant cladding materials.

Identification of optimal substrate preparation methods for chromium coatings development.

Determination of optimal deposition parameters corresponding to the physical methods deposition.

Development of a testing methodology for coated Zy-4 alloy corrosion behaviour evaluation.

Morphological, structural and composition characterization of the chromium coatings.

Measurements of chromium coatings thicknesses, both after deposition and the autoclaving tests.

The evaluation of oxidation kinetics of chromium coatings tested in CANDU primary circuit conditions.

Identification of optimal electrochemical methods, as well as their setting parameters, to assess the anticorrosive properties of the chromium coatings.

Experimental data interpretation and dissemination of research results by reporting of research in scientific articles and attending national and international conferences.

LIST OF SCIENTIFIC WORKS

I.   ARTICLES PUBLISHED IN ISI - INDEXED JOURNALS

1. **Diniași, D.**; Fulger, M.; Butoi, B.; Dinca, PP; Golgovici, F., Accident tolerant barriers for fuel road cladding of CANDU nuclear reactor, Coatings, 2023; **IF: 3,4**

2. Florentina Golgovici, Aurelia Elena Tudose, **Diana Diniași** , Radu Nartiță, Manuela Fulger, Ioana Demetrescu, "Aspects of Applied Chemistry Related to Future Goals of Safety and Efficiency in Materials Development for Nuclear Energy ", Review, Molecules 2023, 28(2), 874, https://doi.org/10.3390/molecules28020874; **IF:4,6/3=1,53**

3. **Diniasi, D.**; Golgovici, F.; Butoi, B.; Fulger, M.; Demetrescu, I. Research on corrosion testing and characterization of protective chromium coatings deposited on Zy-4 substrate. *U.P.B. Sci.Bull.-Series B* **2023**, 85(1), ISSN 1454-2331; **IF:0,5**

4. **Diniasi, D**.; Golgovici, F.; Anghel, A.; Fulger, M.; Surdu-Bob, C.C.; Demetrescu, I. Corrosion Behavior of Chromium Coated Zy-4 Cladding under CANDU Primary Circuit Conditions. Coatings **2021**, 11, 1417, https://doi.org/10.3390/coatings11111417; **IF: 3,2**

5. **Diniasi, D**.; Golgovici, F.; Marin, A.H; Negrea, A.D; Fulger, M.; Demetrescu, I. Long-Term Corrosion Testing of Zy-4 in a LiOH Solution under High Pressure and Temperature Conditions. *Materials* **2021***, 14*, 4586, https://doi.org/10.3390/ma14164586; **IF: 3,748**

II. ARTICLES PUBLISHED IN OTHER DATABASES INDEXED JOURNALS

1. **Diniași, D**.; Anghel, A.; Red, V.; Ion, V.; David, A. Development and characterization of chromium-coating deposited on zircaloy-4 substrate. EMERG vol. VIII, Issue 3/2022, ISSN 2668-7003, ISSN-L 2457-5011;

2. Daniel Petrescu, **Diana Diniași**, Aurelia Tudose, Crina Bucur, "Experimental study of antimony adsorption on magnetite in aqueous solutions", Journal of Nuclear Research and Development, No. 20, May 2021, pp. 56-60, ISSN 2247-191X, ISSN-L 2247-191X;

3. Laurențiu Popa, Mariana Tunaru, **Diana Diniași**, Aurelia Tudose, Lucian Velciu, Mihai Lazăr, "Study of corrosion behaviour of some dissimilar welds from CANDU NPP primary circuit", Journal of Nuclear Research and Development, No. 19, May 2020, pp. 11-17, ISSN 2247-191X, ISSN-L 2247-191X;

4. Mariana Tunaru, Alice Dinu, Laurentiu Popa, Doinita Ciurcu , Aurelia Tudose, **Diana Diniași** , " Use of biocides to prevent the microbiologically induced corrosion of carbon steel pipes " - Short communication, Journal of Nuclear Research and Development, No. 19, May 2020, pp. 18-20, I SSN 2247-191X, ISSN-L 2247-191X.

III. ARTICLES PUBLISHED IN PROCEEDINGS OF INTERNATIONAL DATABASES INDEXED CONFERENCES

1. M. Fulger, M. Tunaru, M. Mihalache, **D. Diniași**, A. Tudose, D. Petrescu, C. Ionescu, L. Popa, "Research Activities in the Frame of National Research Programme "NPP Circuits Chemistry", Nuclear 2021, The 13th Annual International Conference on Sustainable Development through Nuclear Research and Education, May 26-28, 2021, Pitești, România, ISSN 2066-2955;

2. Calin, S.; **Diniași, D** ., Intergranular corrosion testing of 304 L stainless steel, Nuclear 2021, The 13 [th] Annual International Conference on Sustainable Development through Nuclear Research and Education, May 26-28, 2021, Pitesti , Romania , ISSN 2066-2955;

IV. PARTICIPATION IN NATIONAL AND INTERNATIONAL TECHNICAL-SCIENTIFIC CONFERENCES

National conferences

1. **Diniasi, D**.; Demetrescu, I.; Golgovici, F.; Fulger, M.; Tudose A., Corrosion susceptibility of materials used in CANDU systems, Autumn Scientific National Conference of AOSR, November 23-27, 2020, online

2. Aurelia Elena Tudose, Ioana Demetrescu, Florentina Golgovici, Manuela Fulger, **Diana Diniași**, "Coroziunea oțelului inox 310 H în apă în condiții agresive", Conferința Națională Științifică de Toamnă a AOSR, 23-27 noiembrie 2020, on line.

International conferences

1. **Diniasi, D**.; Golgovici, F.; Fulger, M.; Tudose, A.; Alexandru, A.; Demetrescu, I., Comparative Evaluation of the Corrosion Performance of Two Chromium Coatings Deposited on Zy-4 Substrate, International Scientific Conference "Applications of Chemistry in Nanosciences and Biomaterials Engineering - NanoBioMat 2023", 22 - 24 November, 2023, on line

2. **Diniasi, D**.; Demetrescu, I.; Golgovici, F.; Butoi, B.; Tudose A.; Fulger, M., Researches on corrosion testing and characterization of protective coatings deposited on Zy-4 substrate, International Scientific Conference "Applications of Chemistry in Nanosciences and Biomaterials Engineering - NanoBioMat 2022 - Winter Edition", 24 - 26 November 2022, on-line

3. Aurelia Elena Tudose, Ioana Demetrescu, Florentina Golgovici, Manuela Fulger, **Diana Diniaşi**, Cristina Surdu-Bob, Alexandru Anghel, Marius Bădulescu, Oana Brîncoveanu, "Improving Corrosion Resistance of 310 H Stainless Steel Candidate for Generation IV Reactors by Deposition of Chromium Nitride Ceramic Layers", Virtual International Scientific Conference "Applications of Chemistry in Nanosciences and Biomaterials Engineering - NanoBioMat 2022 - Winter Edition", 24 - 26 November 2022.

4. **Diniasi, D**.; Demetrescu, I.; Golgovici, F.; Fulger, F.; Surdu, C.; Anghel, A.; Bădulescu, M.; Tudose A., Application of TVA Coating Technology on Zy-4 Alloy and as-Received Cr Coating Characterization, International Scientific Conference "Applications of Chemistry in Nanosciences and Biomaterials Engineering - NanoBioMat 2021", 25 - 26 JUNE, 2021, on line

5. Aurelia Elena Tudose, Ioana Demetrescu, Florentina Golgovici, Manuela Fulger, **Diana Diniaşi**, Cristina Surdu-Bob, Alexandru Anghel, Marius Bădulescu, "Electrochemical Investigation of Thin CrN_x Films Deposited on 310 H Stainless Steel by Thermoionic Vacuum Arc (TVA) Method", International Scientific Conference "Applications of Chemistry in Nanosciences and Biomaterials Engineering - NanoBioMat 2021", 25 - 26 JUNE, 2021, on line.

V. Books

1. Fulger, M.; **Diniaşi D**.; Tudose, A., Oxidarea în apă la temperaturi supercritice a aliajelor austenitice de grad nuclear, 2023, București, Eikon, ISBN 978-606-49-0846-9

SELECTIVE BIBLIOGRAPHY

[1]   J. Bischoff, C. Vauglin, C. Delafoy, P. Barberis, D. Perche and e. al., "Development of Cr-coated Zirconium Alloy Cladding for Enhanced Accident Tolerance," in *Top Fuel - Light Water Reactor (LWR) Fuel Performance Meeting*, 2016.

[2]   H. Ma, J. Yan and e. al., "Oxidation behaviour of Cr-coated zirconium alloy cladding in high-temperature steam above 1200C," *Materials Degradation ,* 2021.

[3]   F. Iglesias, B. Lewis and e. al., "Clad coolant chemical interaction," NEA-NSC-R--2015-5, Nuclear Energy Agency of the OECD (NEA), 2015.

[4]   D. Diniasi, F. Golgovici and e. al., "Long term corrosion testing of Zy-4 in a LiOH solution under high pressure and temperature conditions," *Materials,* vol. 14, no. 16, p. 4586, 2021.

[5]   D. Diniasi, F. Golgovici and e. al., "Corrosion behavior of chromium coated Zy-4 cladding under CANDU primary circuit conditions," *Coatings,* vol. 11, no. 11, p. 1417, 2021.

[6]   A. Motta, M. Gomes da Silva and e. al., "Microstructural characterization of oxides formed on model Zr alloys using synchrotron radiation," *Journal of ASTM International,* vol. 5, no. 3, 2008.

[7]   A. Motta, A. Couet and R. Comstock, "Corrosion of Zirconium Alloys Used for Nuclear Fuel Cladding," *Annual Review of Materials Research,* vol. 45, pp. 311-343, 2015.

[8]   M. Tupin and F. e. a. Martin, "Hydrogen diffusion process in the oxide formed on zirconium alloys during corrosion in Pressurized Water Reactor conditions," *Corrosion Science,* vol. 116, pp. 1-13, 2016.

[9]   F. Garzarolli, "PWR Zr alloy cladding water side corrosion," *Advanced Nuclear Technology International,* 2012.

[10] C. Huan, W. Xiaoming and Z. Ruiqian, "Application and Development Progress of Cr-Based Surface Coatings in Nuclear Fuel Element: I.Selection, Preparation, and Characteristics of Coating Materials," *Coatings,* vol. 10, p. 835, 2020.

[11] IAEA-TECDOC-684, "Corrosion of zirconium alloys in nuclear power," International Atomic Energy Agency, Vienna, Austria, 1993.

[12] Z. Duan, H. Yang, S. Kano, K. Murakami, Y. Satoh, Y. Takeda and H. Abe, "Oxidation and electrochemical behaviours of Al2O3 and ZrO2 coatings on Zircaloy-2 cladding by thermal spraying," *Surface and Coatings Technology,* vol. 334, pp. 319-327, 2018.

[13] S. Rezaee and G. Rashed, "Electrochemical and oxidation behaviour of yttria stabilized zirconia coating on zircaloy-4 synthesized via sol-gel process," *International Journal of Corrosion,* vol. 2013, p. 9, 2013.

[14] J. Guilemany, J. Fernandez, J. Delgado, A. Benedetti and F. Climent, "Effects of thickness coating on the electrochemical behaviour of thermal spray Cr3C2-NiCr coatings," *Surface and coatings technology,* vol. 153, pp. 107-113, 2002.

[15] D. Diniasi, F. Golgovici, A. Marin, A. Negrea, M. Fulger and I. Demetrescu, "Long-Term Corrosion Testing of Zy-4 in a LiOH Solution under High Pressure and Temperature Conditions," *Materials,* vol. 14, no. 16, 2021.

[16] M. Hirano, T. Yonomoto, M. Ishigaki, N. M. Y. Watanabe, Y. Sibamoto, T. Watanabe and K. Moriyama, "Insights from review and analysis of the Fukushima Daiichi accident," *Journal of Nuclear Science and Technology,* vol. 49, p. 1–17, 2012.

[17] A. Motta and e. a. Capolungo, "Hydrogen in zirconium alloys: A review," *Journal of Nuclear Materials,* vol. 518, pp. 440-460, 2019.

[18] "State-of-the-Art Report on Light Water Reactor Accident-Tolerant Fuels," OECD-NEA, France, 2018.

[19] J. Krejci, J. Kabatova and e. al., "Development and testing of multicomponent fuel cladding with enhanced accidental performance," *Nuclear Engineering and Technology,* vol. 52, no. 3, pp. 597-609, 2020.

[20] J. Thornton, "The microstructure of sputter-deposited coatings," *Journal of Vacuum Science and Technology A,* vol. 4, pp. 3059-3065, 1986.

[21] P. Cantowine and B. Rand, "Irradiation Performance: Light Water Reactor Fuels in Encyclopedia of Nuclear Energy," *Elsevier,* vol. 2, pp. 377-391, 2021.

[22] D. Hussain, "Accident Tolerant Barriers for Fuel Rod Cladding in Nuclear Reactors," *Thesis, Department of Materials Science and Engineering, The University of Sheffield, UK,* 2020.

[23] R. Ozawa, K. Kaykham, A. Hiraishi, Y. Suzuki, N. Mori, T. Yaguchi, J. Itoh and S. Yamamoto, "Field emission from flat metal surfaces covered with Ba atoms," *Applied surface science,* vol. 146, pp. 162-168, 1999.

[24] W. Li and D. Li, "Influence of surface morphology on corrosion and electronic behavior," *Acta materialia,* vol. 54, pp. 445-452, 2006.